QATAR UNIVERSITY

COLLEGE OF ENGINEERING

MECHANICAL PROPERTIES AND DURABILITY OF ULTRA-HIGH-PERFORMANCE CONCRETE WITH LOCALLY AVAILABLE MATERIALS

BY

NEZAM ABDELSALAM ALTAYEH

A Thesis Submitted to

the College of Engineering

in Partial Fulfillment of the Requirements for the Degree of

Master of Science in Civil Engineering

January 2021

COMMITTEE PAGE

The members of the Committee approve the Thesis of
Nezam Abdelsalam Altayeh defended on 24th of Nov. 2020

Dr. Wael Alnahhal
Thesis/Dissertation Supervisor

Dr. Wasim Barham
Committee Member

Dr. Mohammad Irshidat
Committee Member

Approved:

Khalid Kamal A A Naji, Dean, College of Engineering

ABSTRACT

ALTAYEH, NEZAM, A., Master : January : 2021, Master of Science in Civil Engineering

Title: Mechanical Properties and Durability of Ultra-High-Performance Concrete with Locally Available Materials

Supervisor of Thesis: Wael, I, Alnahhal.

Demand for high-rise residential buildings and skyscrapers necessitated the demand for higher strength concrete to reduce the dimensions of concrete structural elements. The rapid deterioration of normal strength concrete under harsh climatic conditions due to deleterious agents' ingress has raised concerns over reinforced concrete (RC) durability in the global construction industry. In the present study, a viable solution to the abovementioned problems, the Ultra-High-Performance Concrete (UHPC) is investigated due to its better mechanical and durability characteristics. Its low porosity and dense microstructures offer high compressive and flexural tensile strengths. Since water and other harmful agents cannot diffuse through the dense structure of UHPC, the durability of RC structures is expected to be enhanced manifolds. UHPC without coarse aggregates are easily fabricated. In this study, a UHPC with similar strength and followability is cast using three types of coarse aggregates up to 12.5% by volume of concrete. Then, the cost of this concrete could be reduced. Also, coarse aggregates make these concrete mixes more viable for the construction industry as for as mixing and shrinkage are concerned. Gabbro, recycled concrete, and steel slag aggregates with the use of micro, macro and hybrid fibers (1% of the volume) are employed to fabricate a 120 MPa in compressive strength after 28 days of curing in UHPC mixes.

The strength is achieved in the following order: steel slag, gabbro, and recycled concrete aggregates UHPCs. It is perceived that compressive strength is increased with steel slag aggregates without losing workability. The durability indicators such as resistivity, porosity, rapid chloride penetration test (RCPT), and sorptivity are also enhanced in all types of UHPC mixes. Using steel slag aggregates in the mix also provides better durability properties and gives higher compressive strength values that other aggregates. Moreover, using macro steel fibers provide high flexural tensile strength results and using micro steel fibers give high compressive strength and durability properties. In addition, using micro and macro steel fiber in the same time gives moderate values in terms of mechanical and durability properties. Also, the addition of fibers enhances the flexural strength more than compressive strength.

DEDICATION

I dedicate this master thesis to researchers and engineers who study the mechanical and durability properties of UHPC.

ACKNOWLEDGMENTS

I would like to thank my supervisors Dr. Wael Alnahhal and Dr. Muazzam Ghous Sohail for their help and efforts to complete this thesis. I would also like to thank Eng. Siju Joseph for his support in conducting several experiments. Without their supervision and support, I would not have been able to complete this research.

TABLE OF CONTENTS

LIST OF TABLES

LIST OF FIGURES

CHAPTER 1: INTRODUCTION

General Background

Conventional Concrete (CC) is a mixture of sand, aggregates, water and cement that require mechanical vibration to reduce air voids and make it flow in formwork during the pouring process. It can be used in many applications like high-rise buildings, bridges and other construction work. The CC has preferred features compared to other materials that are utilized for construction purposes. For example, its raw materials are cheap, easy to fabricate, and could be mold to any architectural shape. Add to that, it is simple to be manufactured. In many cases, it prevents steel bar's rusting for an extended period due to its alkaline environment. However, CC has some weaknesses; for an instant, low tensile strength, high brittle, and inability to absorb energy at failures. Over the last 20 to 30 years, it has been noticed that CC has issues with its durability under harsh environments. It has been highlighted that the estimated cost for repairing deteriorated structures exceeds USD 22.6 billion in the USA [1]. In order to solve these issues, good quality concrete with impervious microstructure is required, the Ultra-High-Performance Concrete (UHPC) is one such concrete.

UHPC is a material known for its positive attributes, such as high compressive and flexural tensile strength and better durability properties. These attributes improve the performance in severe environments, such as high temperature, humidity, and the possibility of sulfate and chloride attack [2-3]. UHPC can be used in many architectural applications that require aesthetics and facades of large structures and structural applications that require high strength such as bridges and nuclear power plants. It has a low amount of water to binder ratio (w/b), equal to 0.2 with a compressive strength exceeding 150 MPa. Tensile strength for UHPC tends to be higher than CC and acts as a brittle material when there is no fiber used in the mix. Fibers such as macro steel,

micro steel, carbon steel, glass, or combinations of these types are commonly used in mixes of UHPC to reach the ductility of the matrix.

Moreover, UHPC has better durability compared with CC due to its higher packing density which leads to smaller crack widths [4]. Adding fibers with the concrete mix provides very low permeability by preventing concrete from chloride attack [5]. In addition, UHPC has a lower amount of voids as it is a heterogeneous material that contains different shapes and sizes of ingredients. The normal size of air voids is between 20 and 50 μm and can reach up to 3 mm. These air voids affect the durability and the strength of the concrete [6]. To achieve a higher strength with lower segregation in the concrete, the voids should be as minimum as possible. Research in this field has been focused on improving the packing density of the concrete matrix in order to improve the mechanical and durability characteristics [7]. The UHPC with higher packing is achieved by using finer materials and removing large aggregates. Nevertheless, there are some issues related to UHPC such as:

- High production cost and lack of control;
- Less amount of available local materials;
- Fewer UHPC standards were established;
- UHPC is sensitive to changes in site conditions;
- Requirement of training for workers and additional equipment for fabrications.

Recently, research in UHPC focuses on achieving the desired mechanical properties using local materials by incorporating supplementary cementitious materials instead of using a high amount of cement, which is considered a high cost [8]. These researches have shown positive signs such as high compressive strength and good ductility and durability [8].

Research Motivations and Significance

Qatar and other Gulf countries suffer from rapid deterioration of reinforced concrete structure after very short service life. Over the years, it is observed that the concrete quality which has been employed is not adequate for severe weather conditions. In order to build resilient infrastructure, the use of high-quality concrete is of utmost importance. In this study, it is decided to fabricate and test the durability of UHPC. The diversity of UHPC makes it possible to be utilized in several construction areas. Architectural and structural applications that require high strength such as bridges and nuclear power plants are examples of possible areas. Moreover, using different coarse aggregate types with a size of 10 mm in diameter is a new subject to explore; they reduce fine materials without impacting the compressive and tensile strength of UHPC. There are high durability properties in UHPC compared to CC, due to the higher density UHPC can offer that shrinks crack widths. Fibers are used in this research to improve the tensile strength instead of using steel reinforcement in the concrete. In addition, a normal curing condition is applied to make sure that UHPC can be cast in site conditions. In general, UHPC gains its strength at an early age and it can be used in prestressed components.

Main Objectives

The main objectives of this research are summarized in the following points:

1. Utilize coarse aggregates with a size up to 10 mm to produce UHPC with a volume of 12.5% of coarse aggregates.
2. Have UHPC mixture using locally available materials (i.e. steel slag aggregates (SSA) and recycled concrete aggregates (RCA) produced from Construction and Demolition Waste (CDW) available in Qatar.
3. Investigate the mechanical properties (compressive and flexural tensile

strengths) and the durability behavior of the produced UHPC.

4. Study the influence of the type of aggregates and fibers on the mechanical properties and the durability of the produced UHPC.

Organization of the Research

Chapter One

This chapter discusses briefly UHPC material background, motivations and significance, and main objectives of this research, as well as the organization of the research and scope of work.

Chapter Two

This chapter presents the state-of-the-art UHPC. It briefs its development history, advantages, manufacturing process, and material properties especially the mechanical properties tests. Moreover, it covers some applications of UHPC and its durability properties.

Chapter Three

This chapter presents materials used in this research: cement, coarse aggregate, fine aggregates, supplementary cementitious materials (i.e. silica fume, fly ash, fibers and superplasticizers). In addition, mixing procedure, curing, and experimental work including the compressive strength, flexural tensile strength, and durability tests: (porosity, rapid chloride permeability test, resistivity, and Sorptivity) are illustrated in this chapter.

Chapter Four

In this chapter, the experimental work results for all specimens are analyzed and discussed to determine each sample’s behavior from compressive, flexural tensile strength and durability tests perspective.

Chapter Five

In this chapter, the main findings drawn from the experimental test results were summarized. Recommendations for future research are also suggested.

CHAPTER 2: LITERATURE REVIEW

Introduction

UHPC is a new generation of concrete that has excellent mechanical properties, workability, and durability compared to normal concrete. Its ingredients are cement, water, fine aggregates, small particles of coarse aggregates, superplasticizers, fly ash, silica fume, and fibers. The purpose of using fly ash and silica fume in UHPC production is to replace some of the cement contents to improve the gradation of materials used in mixes. Many studies on UHPC explore applications that require the use of UHPC such as bridges, precast of bridge girders, and some other structures [9-10].

Silica fume and fly ash are common materials used in UHPC mixes. They are fine materials that provide a high surface area to improve the compressive strength of UHPC [11-13]. Micro steel fibers are the most used material in UHPC [14]. The main role of using fibers in the production of UHPC is to examine its impact on tensile strength [12]. Bache, H. H. (1981) found an improvement in the results of the mechanical properties of UHPC with a 0.2 w/c ratio [14].

Development history

In the 1980s, High-Performance Concrete (HPC) and High Strength Concrete (HSC) were created which resulted in improved compressive strength with a range of 50 to 120 MPa and improved durability. Later, Fiber Reinforced Concrete (FRC) was invented to increase strength, ductility, and crack control improved. During that period, the idea of using fine-grained with homogenous and dense cement was born. It was expected to prevent the spread of microcracks in the structure while loaded [15-16]. Hence, UHPC was invented at that time which was characterized by high compressive strength. Its applications were meant for the security industry such as protective defense

structures. After that, research in UHPC in construction and development started in 1985, which allowed UHPC to be used as a precast element for industrial floors and concrete bridges [17]. Continuous development of UHPC increased the compressive strength of concrete for more than 120 to 200 MPa. Nowadays, the development of UHPC is ongoing and mega-structures are using this concrete type. Buitelaar has made a detailed study on the applications and developments of UHPC in the last 30 years [16].

Advantages of Using UHPC

UHPC has higher durability, better mechanical properties, and higher resistance to environmental attack than CC. Also, using fibers in UHPC has many advantages such as converting it into a ductile behavior instead of a brittle one that is known as concrete behavior, stopping the propagation of cracks, and reducing the crack width, in addition to eliminating the need for steel reinforcement. Fiber has strong compressive and flexural properties to resist the external load effect. Also, UHPC has good resistance to blast, so it is preferred in nuclear plants and high-security areas. It is easier to handle than CC because of its high self-compacting properties. Besides, UHPC has low porosity, which provides higher strength and durability than CC due to the density of the mix.

Manufacturing

While preparing UHPC, some considerations are taken such as mixing speed, temperature of the mix, mixing time, and sequence of mixing to reach a desired property [18]. It is obvious that UHPC has smaller size components than CC. Therefore, it uses different mixing procedures to make sure that the agglomerated tiny particles are mixed well. However, the mixing procedure requires high energy and more time; hence it may overheat.

Graybeal (2006) studied the properties of UHPC after adding superplasticizer on the mix [18]. It took about one hour in mixing time to obtain final workable UHPC. All dry ingredients of UHPC were mixed alone to obtain a homogenous dry mix before the addition of superplasticizer and water. After mixing the dry mix, some pores were filled with water. He concluded that the workability of the mix of UHPC was compromised in results if water and superplasticizer were added before a homogenous dry mix of UHPC. Many researches prepare a UHPC mixture without specific design procedures [20-21].

Sobuz et al. (2016) used specifically graded fine aggregates and complex curing-mixing procedures to trace the complexity in UHPC manufacturing [22]. The forty trials that were undertaken examined the impact of superplasticizer-cement ratio, total-free-water-cement ratio, and fineness on strength and curing procedures of UHPC. The mix was batched in an 80-liter pan mixer. It consisted of sulphate resisting cement, fine and coarse aggregate, silica fume, and steel fibers, and the basic proportions were a ratio of 1:1:0.266:0.233, respectively. The silica fume had a bulk density of 625 kg/m, and the steel fibers yield strength was 1100 MPa.

Four fine aggregates were utilized in his trials: a granulated lead smelter slag, along with a washed river sand, a mined sand, and manufactured sand. The procedure started with mixing all dry components for a minute in the pan mixer until becoming well combined. Then, the water and superplasticizer were added to the pan in varying durations between 7 and 35 minutes subject to the total water content. After that, the fibers were added and mixed for a period of 5 minutes. The final mix was cast in cylinder molds (100x200 mm) and cured in a fog room.

Chen, Y. et al. (2019) demonstrated UHPC mixtures preparation as follows: first added fine and coarse aggregate with cement, silica fume, slag, and limestone

powder and mixed them for 2 minutes in a pan mixer. Then, water with half of the superplasticizer was added for 2 to 2.5 minutes, and the remaining was added after an extra 1 minute. The mixing procedure lasted for 9 minutes until it formed a wet paste. After that, steel fibers were introduced in the mix for a total duration of 15 minutes. Finally, the mix was cast in molds and cured [23].

Alsalman et al. (2017) utilized a 19-Liter pan mixer to mix concrete. The dry mix consisted of cement, sand, silica fume, and fly ash, and mixed for a period of 10 minutes [24]. Then, superplasticizer and water were gradually added to the mix for a total duration of 20 minutes. After that, the mix was poured in cube specimen steel mods of a 50 x 50 mm size. The curing durations were 7, 28, 56, and 90 days.

Durability properties

The definition of durability is the ability of concrete to resist bad weather conditions, chemical attacks, and deterioration process. When a durable concrete is exposed to such bad conditions, it can maintain its serviceability and original form. In recent years, the durability properties of concrete have become a major concern. Although many studies focus on the mechanical behavior of UHPC, durability behaviors are essential to be checked and tested. There are many durability tests for UHPC such as porosity and permeability, chloride ion concentration, concrete resistivity and Sorptivity. Pierard et al. (2012) studied the durability properties of UHPC when exposed to aggressive environmental conditions [25]. Test measures were chloride diffusion, chemical attack, resistance to carbonate, freeze-thaw cycling, and alkali-silica reaction. The results of durability tests indicated an improvement in durability in comparison with normal concrete.

Pores in UHPC samples are low in number and small in size [26-27]. Vernet found that the average pore volume in UHPC is between 1% to 2% and the average size

of the pore is less than 5 nm [28]. The total porosity of UHPC depends on (w/c) ratio and heat treatment. In Vernet's experiment, for example, due to heat treatment, the total porosity of UHPC highly dropped from 8.4% to 1.5% [28]. Roux found that pressuring the specimen during initial setting time reduced the total porosity by 50% [29]. Wang et al. (2012) reported that 0.0005 is the water permeability coefficient of UHPC, and it is three times lower compared to normal strength concrete [30]. Kim Y et al. (2014) showed that when water to cement ratio is high, ordinary Portland cement specimen porosity decreases. For example, increasing water to cement ratio from 0.45 to 0.60 elevates porosity by 150% [31].

Chloride ion penetration is also called the Rapid Chloride Penetration Test (RCPT). UHPC highly depends on water to binder ratio, exposure solution, duration, and curing [24]. Accelerating the test by applying voltage and pressure on samples of UHPC is implemented to evaluate chloride ion penetration depth. For example, Gao et al. (2006) found that the penetration depth is 2.7 mm when applying hydraulic pressure on the UHPC specimen with 1.6 MPa after 128 hours [32]. Roux (1996) mentioned that the chloride diffusion coefficient of UHPC is 2×10^{-14} m^2/s, which is less than normal strength concrete with 1×10^{-12} m^2/s [29]. RCPT can calculate chloride ion penetration by estimating the number of electric charges that pass through UHPC specimen [33]. When performing RCPT, Roux found that using steel fibers in the specimen of UHPC does not cause electrical short-circuiting due to the random distribution and their short length [29]. Furthermore, Mohamed et al. (2015) studied the effect of replacing cement with different volumes of fly ash (0%, 10%, 15%, 20%, 25%, 30%, 35% and 40%) on RCPT test for self-consolidated concrete. Their findings concluded that as the percentage of fly ash increases, RCPT values decrease. RCPT's best value is around 500 coulombs passing through the specimen of replacement of cement with 40% of fly

ash in 40 days of curing. This means that adding more fly ash in the mix enhances the resistance of chloride penetration inside samples rather than using ordinary Portland cement. This reflects the results of RCPT for UHPC by adding half of the volume of cement fly ash and silica fume [34]. Iffat et al. (2017) mentioned that increasing water to binder ratio increases the rapid chloride penetration results. When the range of water to binder ratio exceeds 0.6, RCPT value becomes more than 4000 coulombs (high), whereas when the ratio is between 0.40 up to 0.60, RCPT value falls between 2000 to 4000 coulombs (moderate), however, a ratio less than 0.40 results in a lower RCPT value between 1000 and 2000 coulombs (low), and using UHPC samples gives less than 1000 coulombs (very low and negligible) [35].

The electrical resistivity test measures the quality of UHPC. Polder et al. (2000) stated that there are two processes involved in this test: initiation of the chloride penetration and the propagation of corrosion rate [33]. When the value of resistivity is low, the risk of corrosion elevates. The concept of this test is to measure UHPC resistance by measuring the electric current (I) that passes through UHPC specimen from electrodes and potential difference (V) between two electrodes. Then, resistance in ohms is measured by using measured I and V. Finally, the resistivity (ρ) is calculated in ohm.cm. S. Iffat et al. (2017) studied the effect of two w/b ratios (0.40 and 0.54) of ordinary Portland cement, and a 0.42 ratio of blast furnace slag cement. After 20 years of casting concrete, the resistivity test was conducted to check the risk of corrosion. The resistivity values were 65 kohm.com for the 0.40 w/b ratio of ordinary Portland cement, 120 kohm.cm for the 0.54 w/b ratio, and 345 kohm.cm for the 0.42 w/b ratio of blast furnace slag cement. This means that increasing the amount of binder instead of ordinary Portland cement enhances the electrical resistivity, reducing the risk of corrosion in the future. This reflects the results of resistivity for UHPC by adding half

of the volume of cement fly ash and silica fume [35]. Moon (2013) examined the effect of internal steel fibers on electrical resistivity [36]. It concluded that steel fibers reduce the electrical resistivity of concrete, leading to more corrosion than no-fiber mixes.

Sorptivity is a test that measures the moisture transport of unsaturated concrete samples. Dias (2013) and Patel (2009) emphasized the importance of Sorptivity in testing concrete durability. According to them, it reflects the way that water particles penetrate the concrete and gives an indication for the quality of concrete especially the near-surface ones [37-38]. Moreover, good quality concrete is obtained from low values of Sorptivity. Zhang et al. (2014) illustrated a reduction in compressive strength when water absorption increases [39].

Effect of materials used in UHPC

There are five main materials that are used in the mix of UHPC. These materials are:

- Cement.
- Fine and coarse aggregate.
- Supplementary Cementitious Materials.
- Fibers.
- Superplasticizers.

Cement

Portland cement is the basic binder of the UHPC mix design. The binder content in UHPC is more than CC; therefore, the selection of cement type in UHPC design is critical. Richard et al. stated that using a low amount of calcium aluminates in cement improves the UHPC in terms of mechanical and durability properties [15]. The mechanical behavior of UHPC mainly depends on the type of cement used in the mix. Moreover, the selected type of cement should give high compressive strength using low water content. Bonneau (2002) mentioned coarse cement particles with low C_3A in the

UHPC mix improve workability using less superplasticizer amount than finer cement [40]. Many types of cement are currently used in producing UHPC, however, the types of Portland cement that are most frequently used and recommended are Type I, II and IV [41-42-43-44].

Coarse and Fine Aggregates

The constituents of UHPC should be of high quality because the low ones or weak aggregates affect not only the development of compressive strength, but also the tightness of the packing density. Fine aggregates mainly consist of sand, while coarse aggregates are more of crushed stones. In the case of UHPC, coarse aggregates are typically omitted, and only sand between 150 μm and 4.75 mm is used. Cracks are reduced in a UHPC sample when using a small size of aggregates. Increasing the volume of coarse aggregate leads to reducing both compressive strength and slump flow. Sobuz et al. (2016) stated that curing UHPC for 28 days does not represent the accurate value of compressive strength, and the properties of UHPC are inversely affected if the size of aggregate used in the mix increases [22]. Li et al. (2013) mentioned that using coarse aggregate up to 25% of the total volume used in the mix does not affect the compressive strength results where this percentage is considered as the optimum content [44]. On the other hand, using a high volume of coarse aggregate and fibers gives low efficiency, due to the severe interlock between coarse aggregates and fibers. Ma et al. (2002) researched the effect of using coarse aggregate in the UHPC mix. Two mixes are compared: the first mix is a UHPC with 2-5 mm basalt coarse aggregate, and the second mix is a UHPC without using coarse aggregate. It concluded that using UHPC without coarse aggregate fluidizes the mix easier compared with using coarse aggregate. Therefore, the quality of aggregate used in UHPC mixes should be high to improve the compressive strength. Usually, coarse aggregate is not used in

UHPC mixes, but rather a fine aggregate such as sand is utilized instead with sizes up to 4.75 mm [45].

Supplementary Cementitious Materials

Supplementary Cementitious Materials (SCM) are used in UHPC mixes to replace cement partially. They include fly ash, silica fume, ground granulated furnace slag, and natural pozzolans. Silica Fume (SF) is considered one of the pozzolanic materials that improve concrete properties with an average diameter of 0.15 um. It has more than 90% of SiO_2 and has a high surface area of 15000-25000 m^2/kg. Ibrahim (2017) studied the effect of SCMs on the concrete and its mechanical properties. He concluded that using SF with a volume of 10% to 25% in the mix of concrete increases the compressive strength, while volumes from 25% and 30% [46]. Yoo et al. (2016) stated that the hydration of mixed content using SF is faster than using other types of SCMs. The reason for using SF in concrete mixes is to reduce the content of CO_2 in concrete and make mix cost-effective. Replacing a portion of cement contents with SCMs makes it more friendly to the environment and replaces clinker in cement [47]. Ma noticed that using SCMs in the mix reduces clinker from 85% down to 77% [45]. Randl et al. (2014) found that replacing up to 45% of cement with SCMs in UHPC mix does not affect the mechanical properties of concrete [48]. Ibrahim (2017) conducted an experiment of using GGBS and fly ash as SCMs to replace some volume of cement in the UHPC mix, and his results showed that a 20% replacement improved the properties at the age of 90 days [46].

Fibers

Concrete is a weak material and has restricted post-split conduct with an unexpected failure of the example. The addition of fibers to the UHPC matrix prompts the advancement of UHPC fiber composites. Fiber fortification can possibly upgrade

the tractable execution of UHPC as far as elasticity, pliability, vitality dissemination limit, break separating and split width. Their impact relies on the fiber material and quality, the bond among grid and fiber, the fiber length to width proportion, and the fiber volume division. Because of its high material costs, the measure of strands should be constrained in cost proficient UHPC. UHPC with strands have more noteworthy opposition against high mechanical burdens and natural severe conditions and can improve the solidness and basic obstruction of solid structures [49]. The steel strands are joined into UHPC to conquer any hindrance between the breaks and upgrade the malleability of the material [50]. Richard et al. (1995) suggested that an ideal of a 13 mm long monetary substance and a 0.15 mm distance across steel strands is 2% [15]. According to Wille et al. (2012), an expansion in the network compressive quality, fiber geometry, and fiber volume portion up to a specific range expands the rigidity and elastic endure top pressure esteems [51]. Their findings indicated that a 28-day compressive quality of up to 292 MPa, elasticity up to 37 MPa, and a strain of 1.1% at maximum pressure were seen with a high-quality fiber substance of 8% scattered in a UHPC cementitious blend with no unique warmth or weight treatment. Ibrahim et al. (2017) indicated that by the expansion of 0.65% of strands, the compressive quality improves by 30 MPa [46]. Wu et al. (2016) described that the fuse of a blend of small- and large-scale steel strands could prompt pliable strain solidifying the conduct of the blend [52]. In his experiment, the rigidity of UHPC expanded in a straight way with an expansion of fiber content from 0% to 5% [53]. The consolidation of fiber content from 2-5% increased the chamber compressive quality of example from 3.7% to 25%, while flexural quality expanded up to 100% and shear quality up to 260% compared with no fiber content [54].

The utilization of discrete fiber fortification in UHPC is a need given the weak

idea of the framework. These filaments are dispersed because they increment the flexibility, vitality ingestion, obstruction against delamination and spalling, and exhaustion opposition of the solid lattice. They contain several shapes and sizes and generally described by their proportion of length-to-distance. From materials perspective, the fibers are made of steel or carbon, glass, polyethylene, polyester, polypropylene, and other engineered materials. Steel fibers are mainly categorized into macro and micro materials, where their lengths range approximately between 6 mm and 60 mm and diameter between 0.15 mm and 0.75 mm [47-48-49]. Wille et al. (2012) observed that 1% to 2% of fiber volume is the optimum UHPC utilization [51].

Currently, self-compacting HPC and UHPC blends with steel fibers have been created. Wille et al. (2012) showed that UHPC fiber composites solidified by tractable strain with the elasticity of 13 MPa (1.9 Ksi) can be created by utilizing 1.5 volume percent of high-quality strands. Record rigidity of 15.9 MPa (2.3 Ksi) is accomplished by utilizing just 1.0 volume percent of customized high-quality filaments [51]. Maca et al. (2012) portrayed the plan of UHPC mixes with and without fibers under effect and stun stacking, where the mixes with fibers were planned with a volume of 1% to 3% steel fiber content. A total of 24 mixes were prepared, and the two best performing were selected to study the impact of fiber content. The results showed that 2% and 3% by volume was the ideal measure of filaments regarding mechanical properties and usefulness for the referenced investigation [55].

El-Dieb (2009) researched the possibility of acquiring a self-compacting Ultra High-Quality Cement (UHSC) by utilizing available materials in GCC. USHC compressive and durability were tested. His research findings showed that compressive and split chamber qualities logically expanded along with 0%, 0.08%, 0.12%, and 0.52% steel fiber content. A compressive strength of 123 MPa and flexural strength of

7.2 MPa was obtained after 28 days of curing with a volume of 0.52% [26]. Alkaysi et al. (2015) used concrete, silica fume, fine sand, superplasticizer, and 1% steel fibers to prepare the UHPC mixes. After 28 days of curing, the compressive strength was more than 180 MPa [56]. Azad et al. (2013) structured UHPC utilizing Ordinary Portland Cement (OPC) Type I, fine sand, silica fume, superplasticizer, and 6.3% steel fibers with a diameter of 0.15 mm and a length of 12.7 mm. The mixing time was approximately 14 minutes, and the mixes were first cured at 90°C for 2 days, then sustained inside molds until 28 days before testing. As a result, the compressive strength was 160 MPa and flexural strength was 32 MPa [57]. Graybeal (2006) revealed the effects of several restoring conditions on UHPC with OPC, silica fume, fine aggregate, ground quartz, superplasticizer, and 2% steel fibers with 0.2 mm wide and 13 mm long. The compressive strengths were 193, 174, 172, and 126 MPa. Wille et al. (2012) utilized concrete, silica fume, superplasticizers, and two types of fine aggregates with sizes range between 0.2 mm and 0.8 mm in the mixes. The compressive strength after 28 days varied between 194 MPa and 292 MPa and the flexural strength was in the range of 6.1 MPa to 37 MPa [51].

Superplasticizers

High range water decreasing admixture is essential to accomplish the required functionality of the UHPC blend. Superplasticizers improve the functionality of blend at low water to solidify proportion, henceforth for UHPC where the water to folio proportion is very low, they are important fixing ingredients. Plank et al. (2009) contemplated the impact of two sorts of polycarboxylates (PCEs) on a concrete and silica blend in with low water to solidify proportion [27]. Methacrylate ester copolymers were scattered well in concrete while allyl ether copolymers were scattered well in silica rage. The examination proposed the utilization of a mixed polycarboxylate

copolymer to provide better scattering in both concrete and silica. Ma and Schneider (2002) dealt with the impact of the expansion procedure of superplasticizers in UHPC. The investigation proposed that the stepwise expansion of superplasticizers diminished the blend's consistency and expanded the functionality of the blend. They presented a concrete/superplasticizer blend for which the superplasticizer expansion was not influenced by time; for example, concrete which hydrates gradually [58].

Applications of UHPC

The infrastructure works, building constructions and non-structural products are all potential applications that can benefit from the outstanding performance of UHPC. Its advantage relies on its ability to reduce structures' maintenance due to its good durability properties that sustain more than using normal concrete. Referring to Grand View Research (GVR), the value of UHPC global market size in 2016 was USD 892 million and was expected to reach about USD 1.9 billion in 2025 [59]. UHPC is gaining universal attention with its commercial availability in many countries, such as Australia, New Zealand, Canada, United States, France, Japan, Morocco, Qatar, and South Korea. Extensive research has been steered towards the possibility of industrialization of UHPC as a future sustainable construction material [60].

Here are a few applications that worked from UHPC in subtleties:

Infrastructures

Research and development of UHPC applications in constructions began in 1985 [61]. Since then, different UHPC formulations existed to meet the different requirements of designs, constructions, and architectural approaches. Magog River in Sherbrooke, Canada witnessed the first prestressed hybrid pedestrian bridge that utilized UHPC in 1997 [62]. Later on, it was employed in France in 2001 during the process of replacing corroded steel beams in the severe environment of Cattenom and

Civaux nuclear cooling towers [63-64], and the construction of Bourg-les-Valence bridge [65]. It became clear that the advanced mechanical properties and durability of UHPC were put into consideration to incorporate it with the new designs for many common bridge components. For example, UHPC was used to construct the Seonyu footbridge in South Korea in 2002 with a length of 120 meters [66], making it the longest bridge constructed using UHPC globally. Since then, UHPC bridges' construction for pedestrian traffic has spread in all continents [67].

Buildings and Non-Structural Products

In the last decade, UHPC has been widely used in building components, such as sunshades, cladding, and roof components, due to its ability to produce light, durable, and appealing structures. One of the latest buildings that used UHPC materials is the Foundation Louis Vuitton Pour La Creation in Paris completed in 2014 [68-69], where its high geometric complexity characterized it. Prefabricated UHPC panels were the basis for the cladding designed through vacuum filling molds. Other examples can be illustrated in applications of roofs and canopies, such as the cladding for construction of Qatar National Museum [70]; the roof of Jean Bouin stadium in Paris [71]; and the cladding of Rabat airport Terminal 1 in Morocco [72].

In addition to buildings, UHPC has been regarded as a remarkable resource for non-structural products. It has been broadly used for repairing existing concrete structures, to enhance its mechanical and durability properties which reduces the needed amount of maintenance [73-74]. A bridge over the La Morge River was one of the first structures that required repairing the bridge deck and curbs using UHPC. The results were sustained after one year and no cracks were visible. Similar technologies in bridges were then created such as the hydraulic structures repair and rehabilitation at the Hosokawa River Tunnel in Japan [75].

CHAPTER 3: MATERIALS AND EXPERIMENTAL PROGRAM

This chapter focuses on the materials, sample preparation and experimental program used in this research, to studies the impact of different materials and their volumes on compressive strength, tensile strength, and durability tests.

Materials

UHPC mixes' ingredients are cement, fine aggregate, coarse aggregate, water, superplasticizer, fibers, fly ash and silica fume. Binders used in this research are cement, silica fume and fly ash. Superplasticizers are used in all mixes due to the low w/b ratio. In this research project, the effect of using coarse aggregate and fibers is obtained. More information about all materials used in the production of UHPC is discussed in this section.

Cement

Cement used in this research is manufacture locally in Qatar (Al-Khalij Cement Company for General Purpose Applications). Ordinary Portland cement manufactured by this company is CEM I 42,5 R. It is produced as per the international quality standards. It features a rapid strength growth, a density of 3.11 kg/L, and a specific gravity of about 3.15.

Aggregates

Aggregates used in this research are fine and coarse aggregates. One size of fine aggregates passes through the 600μm sieve and the retained is at 300μm sieve, while the second size passes through 1180μm sieve and the retained at 600μm. For coarse aggregate, the size is up to 10 mm, which is considered as a challenge in this research. Incorporating coarse aggregate in the UHPC mix reduces the cost of production instead of using only fine aggregate. Three types of coarse aggregate were used in the production of UHPC: Steel Slag Aggregate (SSA), Gabbro aggregate (GA), and

Recycled Aggregate (RCA) as shown in Figure 2, 3 and 4. SSA is collected from the production of steel in Qatar Steel Company in Mesaieed Industrial City. RCA is found from Construction and Demolition Waste (CDW).

CDW industry is one of the major solid waste producers worldwide and accounts for 30-40% of the total urban waste generation [76]. In some countries, the annual production of CDW is 10 billion tons; 3 billion of which is produced by China [77], while Europe and the United States generate more than 800 million and 700 million tons [78], respectively. In the next 20 years, Turkey plans to demolish more than 6.7 million tons of its total building stocks for infrastructure transformation. Qatar's situation is similar with the large increase in population, particularly infrastructure works of the 2022 FIFA World Cup and related demolition and construction. Moreover, Qatar's significant growth has recently witnessed, thanks to the foundation of large oil and gas reserves, helped create a large amount of construction, demolition, and excavation waste. Figure 1 shows annual waste generated in Qatar between 2008 to 2012 [79], ensuring that the amount of CDW comprises the largest contribution to the waste produced annually.

Figure 1. Waste generation in Qatar

For all coarse aggregates, several tests were conducted before using them in the UHPC mixes such as Bulk Specific Gravity (BSG) in Dry, Saturated Surface Dry (SSD), Apparent (APP) situations, Absorption (ASTM D570 standard), Flakiness (FK) and Elongation (EL) indices (ASTM D4791 – 19), LA Abrasion (ASTM C131-12 standard), and Soundness (S) Test (ASTM C88 standard). After that, all results are compared with Qatar Construction Specifications (QCS 2014) limits. The physical properties of the used coarse aggregates in UHPC mixes are shown in Table 1.

Table 1. The physical properties of the used coarse aggregates

Type of Aggregate	BSG (Dry) (%)	BSG (SSD) (%)	BSG (APP) (%)	Absorption (%)	FK Index (%)	EL Index (%)	LA Abrasion (%)	S Test (%)
SSA	3.24	3.34	3.48	1.06	1.00	13.00	14.86	0.50
RCA	1.96	2.30	2.13	4.06	6.34	8.00	27.84	-
GA	2.88	2.80	2.93	0.65	8.00	24.00	8.10	2.17
QCS 2014	-	-	-	2	30	35	30	18

Figure 2. Steel Slag Aggregate

Figure 3. Recycled Aggregate

Figure 4. Gabbro Aggregate

By comparing the physical properties in Table 1, the water absorption of coarse aggregate for SSA, GA and RCA are 1.06%, 0.65% and 4.06% respectively, and QCS 2014 standard specifies that the limit of water absorption should not exceed 2%. Since RCA exceeds the limit of QCS 2014, it is important to check its water absorption before 24 hours of using in the mix of UHPC to obtain the desired strength.

The flakiness values are 1%, 8%, 6.34% for SSA, GA, and RCA, respectively, whereas the elongations are 13%, 24%, and 8% for SSA, GA, and RCA, respectively. All figures are within the QCS-2014 boundaries of 30% flakiness and 35% elongation. RCA aggregates have a rough surface and are regarded as heterogeneous and porous. The shape of SSA is quasi-rounding, which eases packing of aggregates in the UHPC mix. It also inhibits the rheological issues due to its greater unit weight.

LA abrasion values, are 14.86%, 8.1%, and 27.84% for SSA, GA, and RCA, respectively, while the LA abrasion limit of QCS-2014 standard is 30%. RCA has the most LA abrasion among aggregates due to the adhered cement mortar on its exterior and the deterioration of aggregates while crushing and demolishing the construction.

The soundness values of SSA and GA are 0.15% and 2.2%, respectively, demonstrating indices within the QCS-2014 standard limit of 18% which make them eligible to use in concrete [53]. Also, a lower soundness value suggests a higher freezing and thawing resistance.

Supplementary Cementitious Materials

In this research, Supplementary Cementitious Material (SCM) is used, such as silica fume and fly ash, shown in Figures 5 and 6. These types of materials are used in UHPC mixes to replace cement partially. Silica fume and fly ash have large surface areas. Adding SCMs to UHPC mix improves its mechanical and durability properties. Grey silica fume is used in the mixes of UHPC while F type of fly ash is utilized. Both are produced by a company called BASF Qatar. The specific gravity of grey silica fume is approximately 2.22 and the average diameter of silica fume is an average of 150 nm. Fly ash has specific gravity of 2.18 and the average diameter is less than 3 μm.

Figure 5. Fly Ash

Figure 6. Silica Fume

Fibers

Concrete is considered a brittle material and the failure is sudden due to the absence of steel reinforcement. Therefore, using fibers in UHPC is essential because of its ability to enhance the tensile concrete strength and reduce crack width, which leads to improved durability properties. Two types of fiber are used in this research to produce UHPC: micro steel fiber and macro steel fiber. The micro is coated with brass while the macro is coated with low carbon, as shown in Figures 7 and 8. The length of micro steel fibers is 12 mm with a 0.2 mm diameter, and the tensile strength is 2,750 MPa. On the other hand, the length of macro steel fiber is 60 mm, with a diameter of 0.75 mm, a tensile strength of 1,225 MPa, and a 200 GPa of modulus of elasticity. The volumes of fibers are 1% for micro steel fibers, 1% for macro steel fibers, and 0.5% for micro and macro steel fibers at the same time.

Figure 7. Micro Steel Fiber

Figure 8. Macro Steel Fiber

Superplasticizer

Using superplasticizer in UHPC mixes is necessary. UHPC mixes require low w/b ratio, therefore adding superplasticizer in the mix enhances the workability of

UHPC. This research's type of superplasticizer is Master Glenium Sky 600 manufactured by BASF Qatar company.

Production and Mixing Procedure

In this section, the production, sample preparation, and curing of UHPC is described.

Mixing Procedure

For the production of UHPC, Portland cement, coarse aggregate, fine aggregate, fly ash, and silica fume are dry mixed in a 90-liter pan mixer. All dry materials are mixed in a concrete mixer for 3 minutes. After that, superplasticizer and water are slowly added, and finally fibers are added to UHPC mix, as shown in Figure 9. The mixing time takes approximately 20 minutes for each mix. Then, all UHPC mix is placed in cylindrical and prism molds. The vibration machine is used for all specimens to remove air voids that happened during the casting of UHPC. After 24 hours of casting, specimens are demolded.

Figure 9. Mixing UHPC Trail

Curing

There is no special technique followed for the curing of UHPC specimens and prisms. All samples are demolded after casting UHPC in 24 hours, then inserted in the water basin. The temperature of the water used in the curing process is approximately 20 degrees Celsius. The two durations for curing UHPC specimens are used 7 and 28 days.

Sample and Mix Preparation

Mix design is important during preparation of UHPC. The particle packing density theory is the basis for improving the workability while casting UHPC, the mechanical properties, and the durability [61]. The design of UHPC mixes is calculated using trial and error method which is preferred in UHPC mix design. Before starting the experimental program for the research, many samples were casted then tested to determine the best combinations and proportions to use. In total, 12 mixes are done in this study with three types of aggregate (SSA, GA and RCA), and each aggregate type includes four mixes such as the control mix (no addition of fibers), using 1% of concrete volume as micro steel fiber, using 1% of concrete volume as macro steel fiber, and mixing both micro and macro steel fibers using 0.5% of the concrete volume of each type. All ingredients of mixes are added based on constant volumes. The volume of the coarse aggregate used is 12.5% of concrete volume. Moreover, w/b ratio is approximately 16%. The main parameters of this study are focused on three types of aggregates with the use of macro, micro steel fibers, and both at the same time, with 1% of binder volume at 7 and 28 days of curing. The specific gravities of all materials are shown in Table 2.

Table 2. Specific Gravity for Materials Used in Mixes

Material Used	Specific Gravity
Portland Cement	3.15
Water	1.00
Fine aggregate	2.67
Recycled aggregate	2.30
Gabbro aggregate	2.80
Steel Slag aggregate	3.34
Silica Fume	2.22
Fly Ash	2.18
Superplasticizer	1.06

The total volume of each mix is assumed to be 0.03 m^3. A total of 102 cylindrical specimens and 24 prism specimens are used. The cylindrical specimens are divided as follows: 36 cylindrical specimens tested for compressive strength at 7 days of curing, and 36 cylindrical specimens tested for compressive strength at 28 days of curing. The 30 remaining specimens are used for durability tests. For the flexural tensile strength test, 24 prisms are casted and prepared. Two mixes (SSA with macro steel fiber and SSA without using fibers) were omitted from flexural tensile strength and durability tests in this research due to a failure that occurred in the flexural tensile machine during the testing process, in addition to other errors occurred during the durability test. Therefore, it was decided to ignore them since the results and the understanding of the mechanical and durability behaviors were expected to remain unaffected. The proportions of all ingredients used for all mixes are shown in Table 3.

In this research, the mixture ID nomenclature is selected based three elements: aggregate, type of fiber, and the fiber fraction in UHPC mix. The first part represents the type of aggregate (SSA, GA, and RCA). The second part identifies the type of fiber being used in the mix, which is illustrated as follows: NSF means no fiber is used, MASF is Macro Steel Fiber, MISF is Micro Steel Fiber, and MAMISF is a mix of macro and micro steel fibers. The last part specifies the percentage of fiber utilized in the mix.

Table 3. Materials Used in Each Mix of UHPC

Material Used	Density (Kg/m^3)	Unit
Portland Cement	770	23.10 kg
Water	177	5.30 L
Fine aggregate (300 μm)	308	9.24 kg
Fine aggregate (600 μm)	154	4.62 kg
SSA	226	6.78 kg
GA	273	8.19 kg
RCA	333	9.98 kg
Silica Fume	193	5.78 kg
Fly Ash	193	5.78 kg
Superplasticizer	11.6	0.35 L
Fiber	18	0.54 kg

The mixtures identification of UHPC based on the type of aggregate and fiber used are shown in Table 4.

Table 4. The Mix Identification of UHPC Used

Mixture ID	Type of aggregate used	Aggregate Volume (%)	Type of fiber	Fiber Fraction
SSA-NSF	SSA	12.50	No fiber used	0.00
SSA-MASF-1%	SSA	12.50	Macro Steel fiber	1.00
SSA-MISF-1%	SSA	12.50	Micro Steel fiber	1.00
SSA-MAMISF-0.5%	SSA	12.50	Both Macro and Micro	0.5 and 0.5
GA-NSF	GA	12.50	No fiber used	0.00
GA-MASF-1%	GA	12.50	Macro Steel fiber	1.00
GA-MISF-1%	GA	12.50	Micro Steel fiber	1.00
GA-MAMISF-0.5%	GA	12.50	Both Macro and Micro	0.5 and 0.5
RCA-NSF	RCA	12.50	No fiber used	0.00
RCA-MASF-1%	RCA	12.50	Macro Steel fiber	1.00
RCA-MISF-1%	RCA	12.50	Micro Steel fiber	1.00
RCA-MAMISF-0.5%	RCA	12.50	Both Macro and Micro	0.5 and 0.5

The mix proportions of UHPC compared to cement mass are shown in Tables 5, 6, and 7.

Table 5. The SSA Mix Proportions of UHPC Compared to Cement Mass

Material Used	SSA-NSF	SSA-MASF-1%	SSA-MISF-1%	SSA-MAMISF-0.5%
Cement	1	1	1	1
Fine aggregate (300 μm)	0.4	0.4	0.4	0.4
Fine aggregate (600 μm)	0.2	0.2	0.2	0.2
FA	0.25	0.25	0.25	0.25

SF	0.25	0.25	0.25	0.25
Water	0.23	0.23	0.23	0.23
SP	0.015	0.015	0.015	0.015
Gabbro	0	0	0	0
SSA	0.125	0.125	0.125	0.125
RCA	0	0	0	0
Micro Steel fiber	0	0	0.01	0.005
Macro steel fiber	0	0.01	0	0.005

Table 6. The GA Mix Proportions of UHPC Compared to Cement Mass

Material Used	GA-NSF	GA-MASF-1%	GA-MISF-1%	GA-MAMISF-0.5%
Cement	1	1	1	1
Fine aggregate (300 μm)	0.4	0.4	0.4	0.4
Fine aggregate (600 μm)	0.2	0.2	0.2	0.2
FA	0.25	0.25	0.25	0.25
SF	0.25	0.25	0.25	0.25
Water	0.23	0.23	0.23	0.23
SP	0.015	0.015	0.015	0.015
Gabbro	0.125	0.125	0.125	0.125
SSA	0	0	0	0
RCA	0	0	0	0
Micro Steel fiber	0	0	0.01	0.005
Macro steel fiber	0	0.01	0	0.005

Table 7. The RCA Mix Proportions of UHPC Compared to Cement Mass

Material Used	RCA-NSF	RCA-MASF-1%	RCA-MISF-1%	RCA-MAMISF-0.5%
Cement	1	1	1	1
Fine aggregate (300 μm)	0.4	0.4	0.4	0.4
Fine aggregate (600 μm)	0.2	0.2	0.2	0.2
FA	0.25	0.25	0.25	0.25
SF	0.25	0.25	0.25	0.25
Water	0.23	0.23	0.23	0.23
SP	0.015	0.015	0.015	0.015
Gabbro	0	0	0	0
SSA	0	0	0	0
RCA	0.125	0.125	0.125	0.125
Micro Steel fiber	0	0	0.1	0.005
Macro steel fiber	0	0.1	0	0.005

Experimental Program

Several standard tests are conducted to evaluate the mechanical and durability properties of UHPC specimens. Compressive and flexural tensile tests are performed. In addition, durability tests are conducted on specimens such as Sorptivity, Porosity,

Resistivity and Rapid chloride Permeability testing (RCPT).

Mechanical Strength Tests

The standard procedure of testing the compressive and flexural tensile concrete strength are described below as follows:

Compressive Strength Test

Six cylindrical specimens from each UHPC mix are tested under compression following ASTM C39/C39M standard. The dimensions of all cylinders are 100 mm in diameter with 200 mm in height. The sample is prepared by removing the excessive moisture. The bearing plate in the compression testing machine is cleaned, then the sample is placed in the center of the plate. The sample is loaded until failure, and then the compressive strength is noted down for each sample from the compression testing machine, as shown in Figure 10. The compressive strength of the mix is taken as the average of 3 specimens for each concrete age.

Figure 10. Compressive Strength Test for Cylindrical Specimen

Flexural Tensile Strength Tests

The flexural tensile strength of UHPC is determined by using a four-point load until failure, as shown in Figure 11. The dimensions of all prisms are 500 mm in length, 100 mm in width, and 100 mm in height. Three prisms of each mix are tested. All prisms are tested as displacement control at a rate of 0.1 mm/min. A graph plotted for a relationship between compression load (KN) and displacement (mm). Flexural tensile strength, toughness and relative flexural strength can be determined by using the calculation method in the ASTM C1609/C1609M standard.

Figure 11. Flexural Tensile Strength Test for Prism Specimen

Durability

There are four main durability tests on all trail mixing of UHPC: resistivity test, porosity test, rapid chloride penetration test, and sorptivity test. In total, 30 cylindrical specimens are tested. Specimen preparation for porosity, rapid chloride penetration and sorptivity tests are done after finishing resistivity test by cutting cylindrical specimens into three equal pieces to be 50 mm in height as shown in Figure 12. All samples are dried in an oven until the dry mass of each specimen is constant.

Figure 12. Specimens Preparation for Durability Tests

Resistivity

The resistivity test is used as an indicator of the resistance of chloride penetration ions through UHPC samples. The reason for testing specimens of UHPC with electrical resistivity tests is to measure the quality of UHPC; when the value of resistivity is lower, the risk of corrosion becomes higher. All UHPC samples are prepared by placing them inside large tanks for three days before starting the experiment. After that, the Surface Electrical Resistivity Meter (SERM) device is used to calculate the resistivity results of each specimen as shown in Figure 13. The standard used for the resistivity test is AASHTO TP 95.

Figure 13. SERM Device

Porosity

The purpose of this test is to measure the volume of voids in UHPC specimens. Firstly, all specimens are cut into smaller sizes (50 mm in height) and dried in an oven for 24 hours. Then, the mass of each specimen is calculated, and the process is repeated until the difference in masses is less than 0.5%. After that, all specimens are submerged in water for approximately 30 minutes and the masses are recorded. The volume of voids is calculated by the difference in dried and submerged specimens' masses. The standard used for the porosity test is ASTM C1754/C1754M.

Rapid Chloride Penetration Test

Rapid Chloride Penetration Test (RCPT) is a test that measures the transfer of a charge through the UHPC surface and based on the result, the quality of the UHPC sample is known. One of the leading causes of corrosion of steel fibers or reinforcement is chloride ions penetration. There are many chloride sources such as irrigation water and industrial water, which leads to corroding the UHPC. All specimens are dried in an

oven at 50°C for at least 3 days. All samples are coated with silicone from the sides of specimen. Then, all samples are placed in a desiccator under vacuum for three hours at 50 mmHg pressure. After that, water fills the desiccator until all samples are fully submerged with approximately one hour. After 18 hours, samples are inserted in the RCPT device shown in Figure 14. On one side, sodium chloride solution with 3% concentration is added, and 0.3% concertation of sodium hydroxide is added on the other side. The results of all samples are recorded for the initial time and for each half an hour until reaching 6 hours. This test follows the ASTM C1202 standard.

Figure 14. The Setup for RCPT Device

Sorptivity

Sorptivity test is used to determine the rate of water absorption in UHPC by capillarity suction, where the absorption is plotted with the function of time. In this test, all specimens are dried until they reach a constant dry mass and coated with silicon.

After that, all samples are kept at room temperature and sealed to ensure that all specimens have the same condition for 15 days. Before starting the test, dry mass for each sample is recorded. The water level has to reach a range of 2 mm from the bottom side of each sample, as shown in Figure 15. In addition, all samples are immersed in water for a specific time to know the absorption rate of water for UHPC based on the ASTM C1585 standard. Many factors affect sorptivity tests such as mix proportions of UHPC, entrained air voids content, duration, type of curing, and presence of micro cracks in samples.

Figure 15. Setup for Sorptivity Test

CHAPTER 4: RESULTS AND DISCUSSION

In this section, all results of experimental tests including compressive strength, flexural tensile strength, porosity, resistivity, RCPT, and sorptivity tests are listed and discussed in detail. The comparisons of all mixes are illustrated in order to decide which types of aggregates and fibers are preferred to produce a high quality of UHPC in terms of mechanical and durability properties.

Mechanical Properties

The results of the compressive and flexural tensile strength of UHPC mixes are shown in Tables 8 and 9. The compressive strength is calculated for both 7 days and 28 days of curing, while the flexural tensile strength is calculated for 28 days of curing only. The flexural tensile strength, toughness, and relative flexural strength values are calculated using the compression load and displacement graph based on ASTM C1609/C1609M standard. Each value represents the average of 3 samples for each mix.

Table 8. The Results of Compressive Strength of UHPC at 7 and 28 Days

Mixture ID	Age of UHPC	Compressive Strength (MPa)
SSA-NSF	7 Days	124.9
	28 Days	142.3
SSA-MASF-1%	7 Days	122
	28 Days	138.1
SSA-MISF-1%	7 Days	134.2
	28 Days	156.8
SSA-MAMISF-0.5%	7 Days	125.9
	28 Days	157.0
GA-NSF	7 Days	115.8
	28 Days	137.3
GA-MASF-1%	7 Days	118.9
	28 Days	136.3
GA-MISF-1%	7 Days	115.2
	28 Days	140.7
GA-MAMISF-0.5%	7 Days	125.5
	28 Days	147.1
RCA-NSF	7 Days	109.2
	28 Days	128.5
RCA-MASF-1%	7 Days	114.8

	28 Days	134.7
RCA-MISF-1%	7 Days	109.4
	28 Days	139.9
RCA-MAMISF-0.5%	7 Days	117.6
	28 Days	147.1

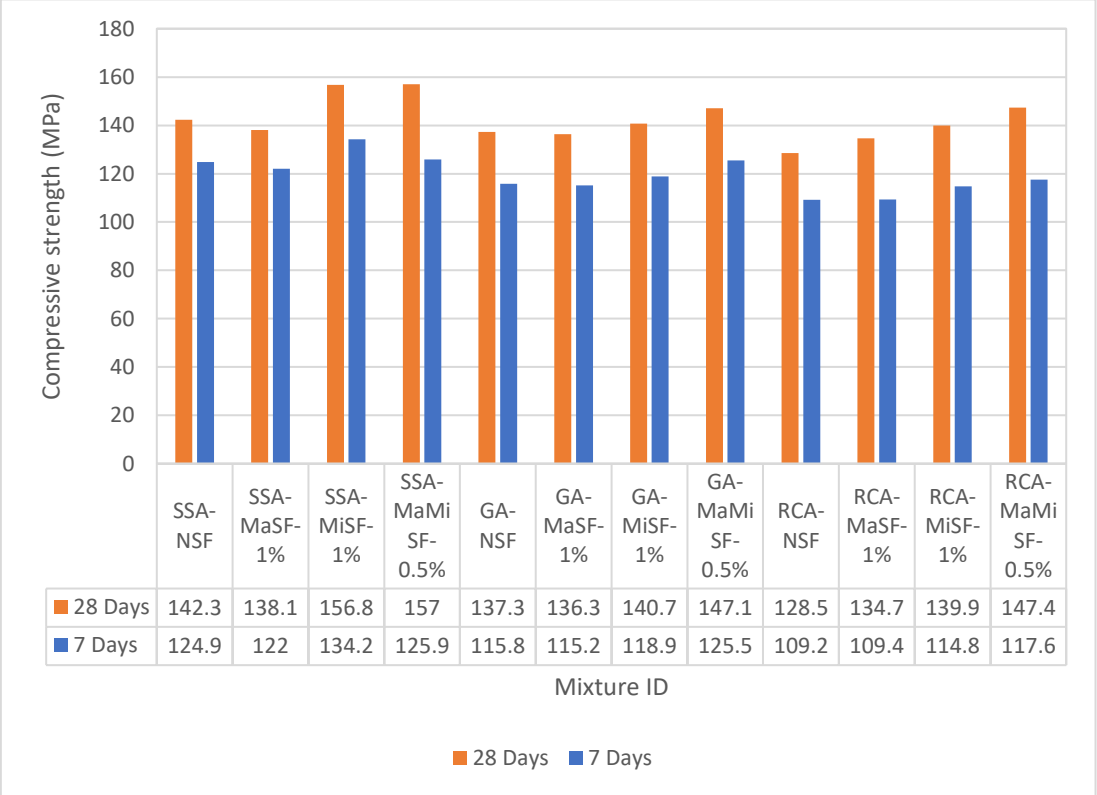

Figure 16: Compressive strength at 7 and 28 days of curing

Values recorded from the average compressive strength test after 7 and 28 days of curing are shown in Figure 16.

Compressive Strength After 7 Days of Curing

The maximum compressive strength obtained within 7 days of curing among all types of aggregates is SSA-MISF-1%, which is 134.2 MPa as shown in Figure 16, while the lowest compressive strength is RCA-NSF with the value of 109.2 MPa. By looking at the mixes' groups, SSA-MISF-1% has the highest value among SSA mixes. Also,

the strength of GA-MAMISF-0.5% mix is the highest among GA mixes, and the strength of RCA-MAMISF-0.5% surpasses other RCA mixes.

For control mixes with no steel fiber (SSA-NSF, GA-NSF, and RCA-NSF), SSA-NSF leads the comparison with a value of 124.9 MPa. Moreover, the difference between SSA-NSF and GA-NSF is 9.1 MPa compared to 15.7 MPa between SSA-NSF and RCA-NSF. The highest value among micro steel fiber mixes is the 134.2 MPa of SSA-MISF-1% and it is more than GA and RCA samples by 15.3 MPa and 19.4 MPa, respectively. The reason behind this is that SSA possesses the highest specific gravity value of 3.24 compared to 2.88 in GA and 1.96 in RCA. Moreover, SSA surface has an extensive pore network and substantial rough surface. These large pores impact the Interfacial Transition Zone (ITZ) by creating a dense ITZ between the aggregate and its surrounding components. The rough aggregate surface provides better interlocking with the UHPC component. The improved strength of GA makes it the second-best aggregate after SSA in terms of compressive strength because its angularity produces enhanced interlocking properties compared to RCA. Hence, the least compressive strength is produced by RCA at the same mixture proportions compared to GA and SSA, since it has a poor mortar layer caused by demolishing old structures. Each time RCA is reused after being demolished results in a degraded mechanical behavior.

The combination of both macro and micro steel fibers in UHPC mixes resulted in the highest compressive strength values among all types of aggregate. For instance, the effect of micro steel fibers can be expressed by GA mixes. GA-MAMISF-0.5% has a compressive strength value more than GA-MISF-1%, GA-NSF and GA-MASF-1% with an increasing percentage of 5.26%, 7.73% and 8.21%, respectively. Using the combination between micro and macro steel fibers enhances the compressive strength compared to macro steel fibers because micro steel fiber reduces the crack width, makes

the UHPC sample denser, and reduces the voids. Moreover, the presence of macro with micro steel fibers in the mix provides more compressive strength than using micro steel fiber only; the macro steel fiber provides more compressive strength without reducing the packing density due to having micro steel fiber in the UHPC mix. Using macro steel fiber also increases the ratio of the pore due to its long length and diameter, which reduces the compressive strength. It is noticed from the graph that SSA with the use of micro steel fiber at 7 days of curing is the only sample that exceeds the hybrid fibers sample. Therefore, the mechanical properties of SSA overcome the effect of fibers in compressive strength. Although it impacts compressive and flexural tensile strength, the enhancement in the tensile straining capacity is significantly better than the compressive strain capacity.

Compressive Strength After 28 Days of Curing

The SSA-MAMISF-0.5% mix has the maximum compressive strength of 157 MPa after 28 days of curing as shown in Figure 19, while the lowest compressive strength belongs to mix RCA-NSF with a value of 128.5 MPa. It is noticed that using the combination of macro and micro steel fibers with SSA, GA, or RCA mixes contributes to a better compressive strength in the 28 days (SSA-MAMISF-0.5%, GA-MAMISF-0.5%, and RCA-MAMISF-0.5%). It is also noticed that utilizing SSA in any type of mix significantly improves the compressive strength of the mix. For instance, SSA-NSF resulted in a higher value of compressive strength compared with GA-NSF and RCA-NSF. The same applies to the mixes of SSA-MASF-1%, SSA-MISF-1%, and SSA-MAMISF-0.5% compared with other mixes.

Overall, the values show improved compressive strengths in the 28-day period of curing in all types of aggregates and fibers, which is similar to the 7-day period. However, the 28-day period resulted in an average difference of 20 MPa higher than

the 7-day period. Such an increase has resulted from the effect of the hydration process in the UHPC matrix.

Flexural Tensile Strength

Flexural tensile strength test results of UHPC mixes after 28 days of curing are presented in Table 8 and shown in Figure 17. Flexural tensile strength is a relationship between the compression load (KN) with displacement (mm) that is plotted in a graph to determine the flexural tensile strength, toughness, and equivalent flexural strength ratio by using ASTM standard C1609/C1609M. The toughness (Joule) can be obtained by calculating the area under the curve of compression load and displacement relationship. Equivalent flexural strength (MPa) is calculated from the average of compressive load applied on a sample up to 3 mm of displacement. In this section, the flexural behavior of each mix is discussed.

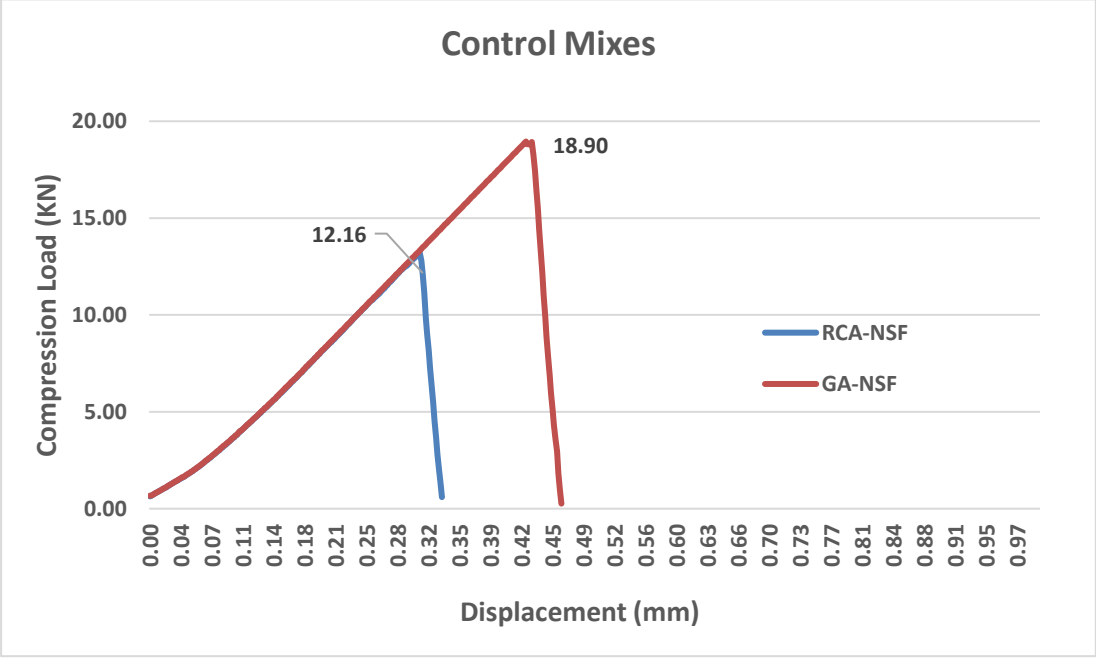

Figure 18. Flexural Behavior for Control Mixes

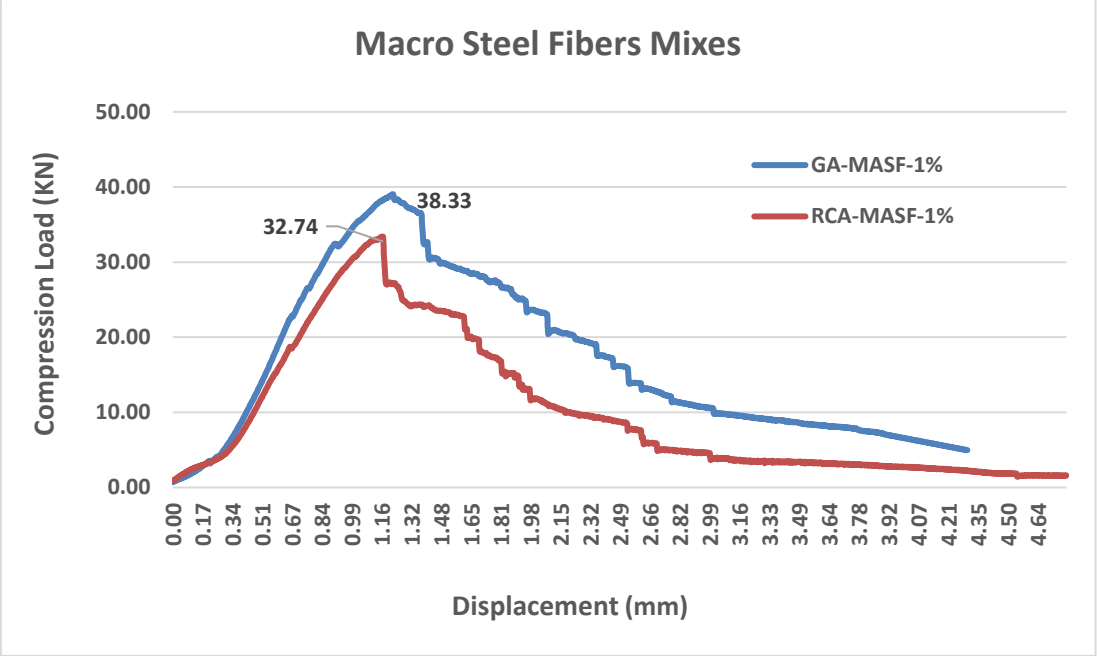

Figure 19. Flexural Behavior for Macro Steel Fibers Mixes

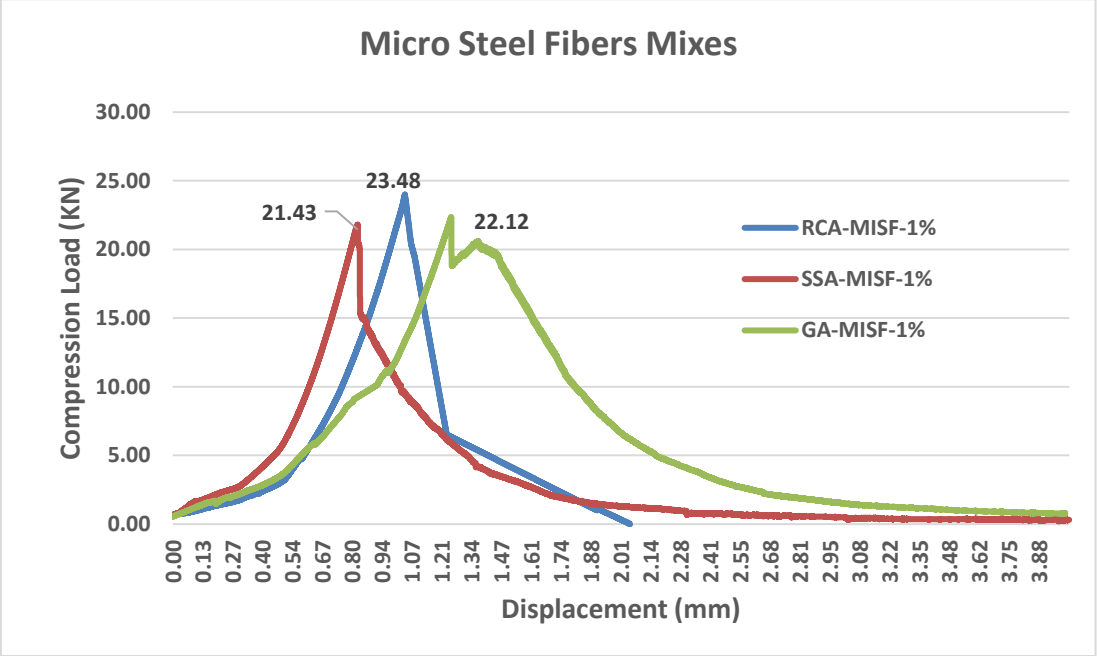

Figure 20. Flexural Behavior for Micro Steel Fibers Mixes

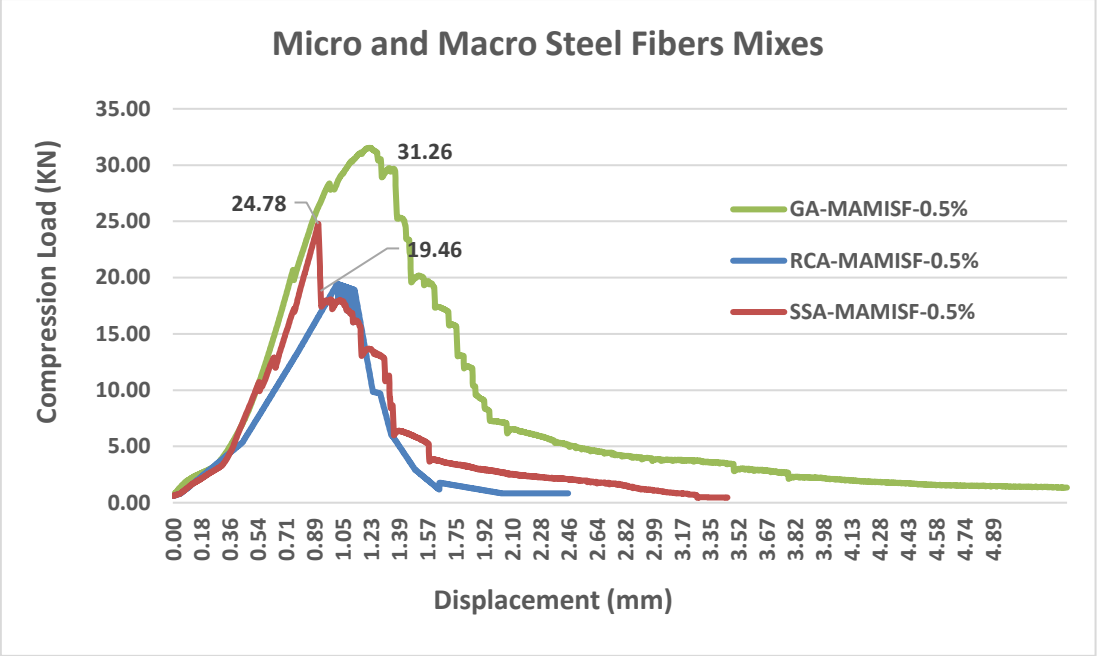

Figure 21. Flexural Behavior for Micro and Macro Steel Fibers Mixes

In general, the flexural behavior of any sample tolerates compression force until it reaches the maximum sustainable load. In this stage, the behavior changes from elastic to plastic, which indicates occurring of deformation, and the specimen do not retain back as before. After that, compression load starts to decrease until the sample breaks. In the elastic region, stiffness is determined by calculating the slope of the line. It is noticed that the fiber gives the UHPC mix a stiffness more than no usage of fiber in the mix. Increasing the size of fiber provides a better stiffness. Also, the fiber effect is observed through the zigzag lines, therefore fibers convert the behavior of UHPC from brittle to ductile. Control Mixes do not resist the force upon reaching maximum compression load and breaks immediately due to the absence of fibers. It is noted from Figures 18,19,20 and 22 that Macro steel fiber produces UHPC with higher flexural strength, equivalent flexural strength, and toughness. Hybrid fibers have a moderate effect between macro and micro steel fibers alone. Finally, control specimens have the lowest toughness, flexural strength, and equivalent flexural strength.

Table 9. Results of flexural strength test

Trail Mix	Maximum Load (KN)	Flexural Tensile Strength (MPa)	Toughness (J)	Equivalent Flexural Strength (MPa)
SSA-MISF-1%	21.43	10.72	21.43	3.92
SSA-MAMISF-0.5%	24.78	12.39	30.98	6.66
GA-NSF	18.90	9.50	9.45	0.42
GA-MASF-1%	38.33	19.17	63.82	21.18
GA-MISF-1%	22.12	11.06	32.07	4.23
GA-MAMISF-0.5%	31.26	15.63	46.89	12.91
RCA-NSF	12.16	6.08	1.95	0.30
RCA-MASF-1%	32.74	16.37	54.02	14.72
RCA-MISF-1%	23.48	11.74	17.95	2.84
RCA-MAMISF-0.5%	19.46	9.70	12.65	4.27

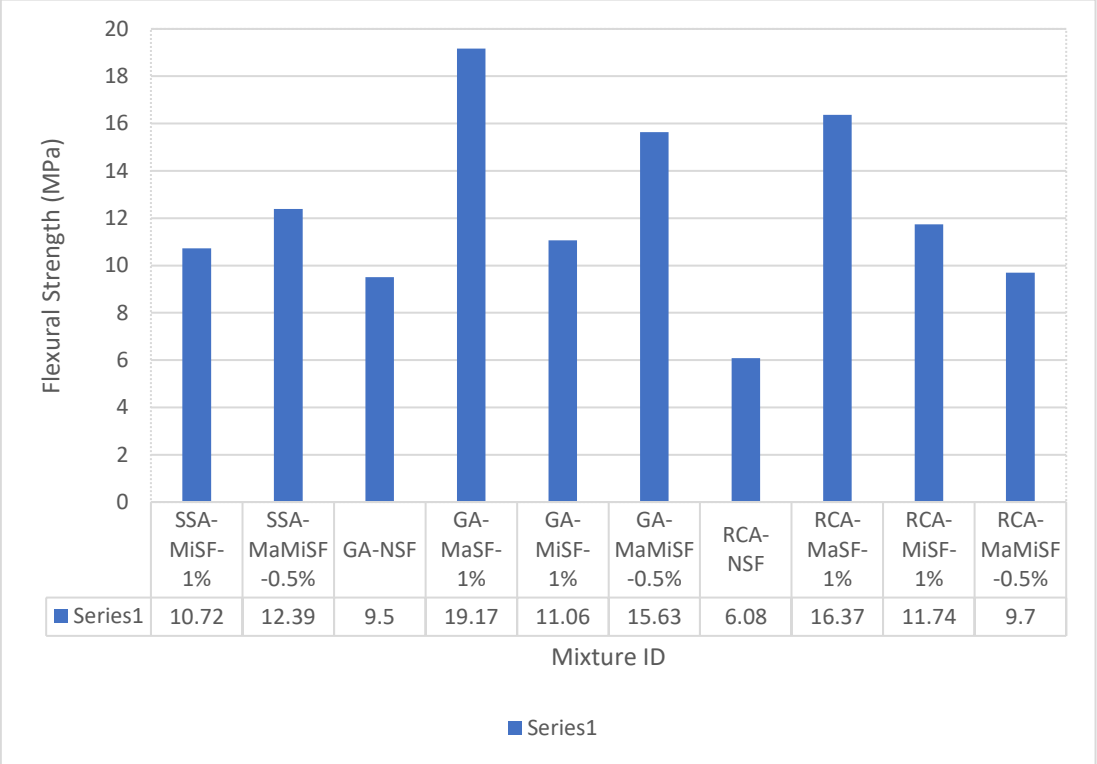

Figure 17: Flexural Tensile Strength for 28 Days of curing

The maximum compression load value is in GA-MASF-1% at 38.33 KN, where it reaches 5 mm displacement without break. Its flexural tensile strength is 19.17 MPa, the toughness is 63.82 J, and the equivalent flexural strength is 21.18 MPa. The least compression load value is in RCA-NSF at 12.16 KN, which is less than 1 mm displacement, and the flexural tensile strength is 6.08 MPa, the toughness is 1.95 J and equivalent flexural strength is 0.3 MPa. The values of toughness and equivalent flexural strength depend mainly on the behavior of flexural strength before 3 mm approximately. For the flexural behavior of control mixes, GA-NSF and RCA-NSF share the same behavior of flexural strength; they suddenly break after reaching their maximum compression loads due to the absence of fiber in the mixes. GA-NSF sample has more flexural strength, toughness and equivalent flexural strength values than RCA-NSF with 3.42 MPa, 7.8 Joule, 0.12 MPa respectively. The break happens in ITZ which is the weakest point in the sample. GA has better ITZ than RCA due to its lesser void content in the aggregate, in addition to being more angular and rougher. Also, RCA has poor mortar on aggregate surface due to the demolishing of old structures that increases the void content which reduces its mechanical properties.

The effect of fibers is observed in flexural tensile strength. Table 10 illustrates the differences in flexural tensile strength, toughness, and equivalent flexural strength between GA-MASF-1% and the other GA mixes: GA-MISF-1%, GA-MAMISF-0.5%, and GA-NSF.

Table 10. Characteristic comparison between GA-MASF-1% and Other GA Types

Aggregate Compared with	Flexural Tensile Strength	Toughness	Equivalent Flexural Strength
GA-MISF-1%	8.11 MPa	31.75 J	16.95 MPa
GA-MAMISF-0.5%	3.54 MPa	16.93 J	8.27 MPa
GA-NSF	9.67 MPa	54.37 J	20.76 MPa

It is noticed that using micro steel fiber in the mix does not enhance the flexural tensile strength compared with macro steel fiber. However, macro steel fiber is characterized by its long length and wide width compared to micro steel fibers, which makes it capable of absorbing stresses caused by the external force and reduces cracks propagation. Also, the number of fibers per unit volume of UHPC leads to more fibers bridging cracks. The combination of macro and micro steel fibers at the same time give moderate results due to having a small and big size of fibers at the same time.

Compressive Strength Test vs. Flexural Tensile Strength Test

Table 11 shows compressive strength and flexural tensile strength results for all UHPC mixes after 28 days of curing. In this section, a comparison between mechanical tests are discussed.

Table 11. Values of Compressive and Flexural Strengths

Trail Mix	Compressive Strength (MPa)	Flexural Tensile Strength (MPa)
SSA-NSF	142.3	NA
SSA-MASF-1%	138.1	NA
SSA-MISF-1%	156.8	10.72
SSA-MAMISF-0.5%	157	12.39
GA-NSF-1%	137.3	9.5
GA-MASF-1%	136.3	19.17
GA-MISF-1%	140.7	11.06
GA-MAMISF-0.5%	147.1	15.63
RCA-NSF-1%	128.5	6.08
RCA-MASF-1%	134.7	16.37
RCA-MISF-1%	139.9	11.74
RCA-MAMISF-0.5%	147.4	9.7

As shown from Table 11, SSA mixes lead the comparison in higher compressive strength while GA mixes exceed others in flexural tensile strength values. This is because both SSA and GA have high physical properties in terms of specific gravity

and lower LA abrasion, flakiness and elongation index compared with RCA. However, RCA is not a virgin aggregate and is not used in structural buildings, therefore it has low mechanical properties.

Micro steel fiber enhances the compressive strength more than macro steel fibers due to their short length and small diameter, which makes the mix denser and with lower voids content. On the other hand, using macro steel fiber gives better values for flexural tensile strength because of the fiber size and its characteristics, which eases the bridging effect of fibers and carry the stresses away from the easily breakable ITZ.

For macro and micro steel fiber results, it shows moderate improvement for both mechanical properties. Although the combination of both fibers does not generate the best outcome, it still provides acceptable results for compressive and flexural tensile strength at the same time.

Finally, the brittle behavior of UHPC is observed in flexural tensile strength which is easily breakable without any signs. Moreover, using fibers in the UHPC mix results in more improvement in flexural strength than in compressive strength. The maximum improvement percentage of using fibers in flexural strength is approximately 50% in GA-MASF-1% in comparison with GA-NSF. For compressive strength, the improvement percentage of SSA-MISF-1% sample is 9.25% compared with SSA-NSF.

Durability Tests

In this section, the four durability tests (resistivity, porosity, RCPT, and sorptivity) are implemented to study the effect of different aggregates and fibers used in UHPC mixes. All test results are shown in Table 12.

Table 12. All Durability Results

Mixture ID	Resistivity (KOhm.Cm)	Porosity (%)	RCPT (C)	Initial Absorption ($mm/s^{1/2}$)	Secondary Absorption ($mm/s^{1/2}$)
SSA-MISF-1%	487.88	0.86	17	0.011	0.0036
SSA-MAMISF-0.5%	278.41	1.46	31	0.0166	0.0041
GA-NSF	464.20	2.31	72	0.0282	0.0027
GA-MASF-1%	148.10	3.41	151	0.0297	0.0036
GA-MISF-1%	344.62	1.51	48	0.0259	0.0091
GA-MAMISF-0.5%	254.21	1.92	68	0.0277	0.005
RCA-NSF	167.07	2.17	127	0.0194	0.005
RCA-MASF-1%	149.54	2.19	149	0.0196	0.005
RCA-MISF-1%	333.89	1.44	32	0.0139	0.0036
RCA-MAMISF-0.5%	340.82	1.70	35	0.0125	0.0041

Resistivity

The resistivity test calculation depends on certain constant parameters. These parameters are as follows: 10 cm radius of each sample, 314 cm of cross-sectional area, 20 cm length, and 15.7 cm of geometrical factor (K) that depends on the sample area and length. The geometrical factor is calculated by dividing the cross-sectional area by the length using the SERM device. The results represent the average of three specimens. All samples are kept in saturated condition to eliminate the effect of humidity. Resistivity is then calculated by multiplying the geometrical factor by average resistance. This test follows the standard of AASHTO-95-TP.

The resistivity test classifies the chloride ion penetration into different levels. When the resistivity value is more than 254 kohm.cm, the chloride ion penetration is considered as negligible. A very low chloride ion penetration is determined when the resistivity of electricity is from 37 kohm.cm up to 254 kohm.cm, whereas for low, moderate and high levels of chloride ion penetration resistivity is between 21 and 37 kohm.cm, 12 and 21 kohm.cm, and less than 12 kohm.cm, respectively. Corrosion is also classified based on the resistivity value. When concrete resistivity is less than 10

kohm.cm, the risk of corrosion is high, but it is considered moderate in the range of 10 and 50 kohm.cm and becomes low when concrete resistivity is between 50 and 100 kohm.cm. Values more than 100 kohm.cm of resistivity makes the risk of corrosion negligible.

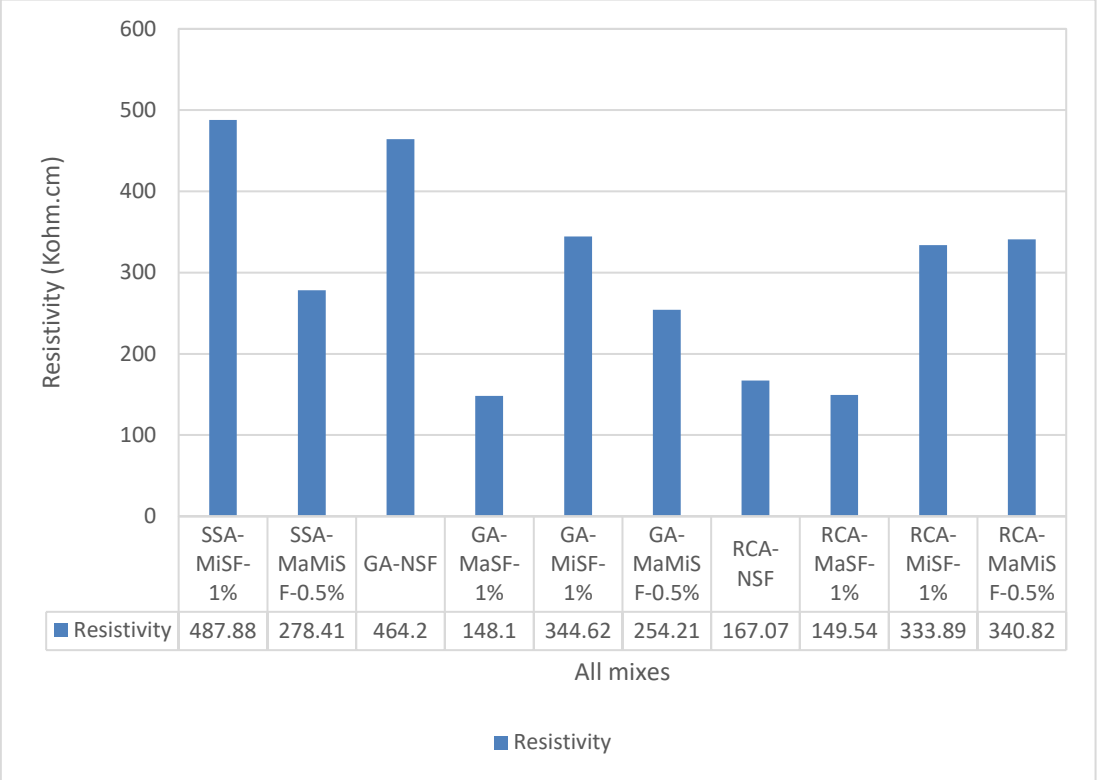

Figure 22. Resistivity of All Samples

By looking at the results in Figure 22, the highest resistance value of electricity is SSA-MISF-1% with a value of 487.88 kohm.cm, whereas the lowest value of electricity that passes through the specimen is GA-MASF-1% with 148.1 kohm.cm. It is noticed that all samples exceed 100 kohm.cm, which means that they possess a negligible risk to corrosion.

For control specimens, GA-NSF has a higher resistance compared to RCA-NSF with a difference of 295.13 kohm.cm, which indicates that GA resists more electricity and has a lower possibility of being corroded than RCA. In addition, SSA-MISF-1%

has a high resistivity value compared with GA-MISF-1% and RCA-MISF-1% by 29.35% and 31.56%, respectively. This is because SSA and GA properties have lower void ratios and water absorption than RCA that affect directly the flow of electrical charge through the sample. Also, SSA has low electrical conductivity and its effect is negligible.

On the other hand, GA-MISF-1% increases the resistivity value by 90.41 kohm.cm compare to GA-MASF-1%, therefore, macro steel fiber reduces resistivity in all types of aggregate due to its conductive properties and voids increase in samples, since the use of long length fibers transfers electricity easier than micro steel fiber. This leads to high levels of corrosion in macro steel fibers mixes for all types of aggregate. In case of using 1% of micro steel fibers, SSA-MISF-1%, GA-MISF-1%, and RCA-MISF-1% all have high electrical resistance values of 487.88 kohm.cm, 344.62 kohm.cm, and 333.89 kohm.cm, respectively. This means that using micro steel fiber in SSA results in a lower risk of corrosion because it makes the mix denser than GA and RCA. Also, the effect of micro steel fibers in packing density is more than conducting electricity due to its small size. Similarly, with 0.5% of both macro and micro steel fibers, RCA-MAMISF-0.5% has a moderate electrical resistance and possibility for corrosion compared with RCA-MISF-1% and RCA-MASF-1%.

Porosity

Similar to resistivity, the porosity test calculation depends on certain constant parameters represented as follows: the diameters of all samples are 101 mm, and the temperature of water is 18.8 degrees Celsius, which means that the water density is equal to 998.21 kg/m^3. This test follows the standard of ASTM C1754/C1754M. Before the test, all samples were prepared to be 50 mm in height and dried in an oven until the dry masses are fixed.

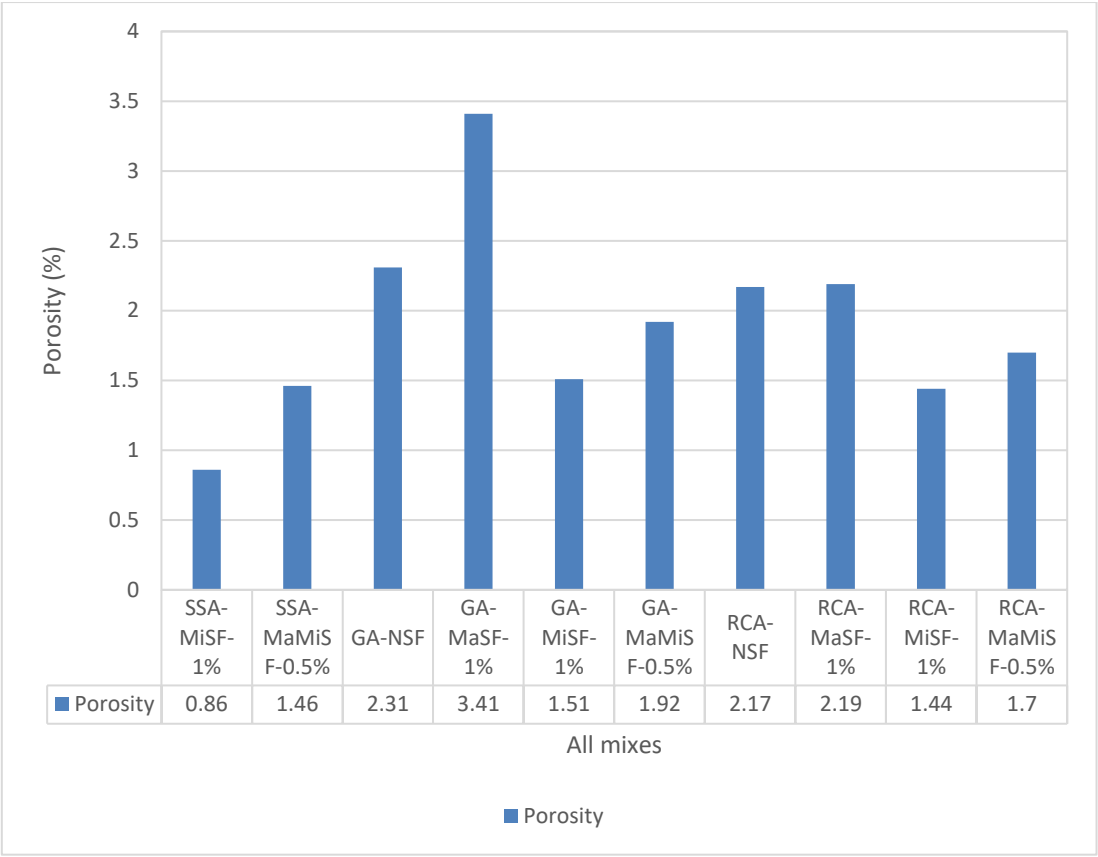

Figure 23. Percentage of Porosity for All Samples

As shown in Figure 23, the highest void ratio percentage is GA-MASF-1% with 3.41%, while the lowest void ratio percentage is SSA-MISF-1% with 0.86%. For control specimens, GA-NSF has a high porosity ratio compared with RCA-NSF by 0.14%. Also, it is noticed that SSA-MISF-1% gives a low porosity ratio of 0.86% compare with GA-MISF-1% and RCA-MISF-1% with values of 1.51% and 1.70%, respectively. Also, SSA has a high packing density than GA and RCA. Hence, it is clearly observed that SSA provides a dense mix that reduces the voids to the minimum.

The effect of fibers appears when comparing GA-MISF-1, GA-MAMISF-0.5%, and GA-MASF-1%. Micro steel fiber sample has lower pores ratio than the hybrid and macro steel fiber samples by 0.41% and 1.90%, respectively, because it reduces the crack width and do not affect the packing density of sample, while using macro steel fiber in UHPC mix reduces the interaction between UHPC materials and

the fiber itself, which leads to an increase in the number of voids in samples due to its long length and its wide diameter. Moreover, using 0.5% of both macro and micro steel fibers has moderate values in terms of porosity percentage in samples.

RCPT

This test follows the standard of ASTM C1202. Before the test, all samples are prepared to be 50 mm in height and dried in an oven until the difference between pre- and post-heating is 0.5% or less, which then is used in RCPT machine. The duration of test is 6 hours where readings are recorded for each sample every 30 minutes. Chloride ion penetrability levels follow the ASTM C1202 standard. When RCPT value is less than 100 coulombs, the chloride ion penetration is considered negligible. Very low level of chloride ion penetration is determined when the RCPT value is between 100 and 1000 coulombs. For low, moderate and high levels of chloride ion penetration, RCPT falls between 1000 and 2000 coulombs, 2000 and 4000 coulombs and exceeds 4000 coulombs, respectively.

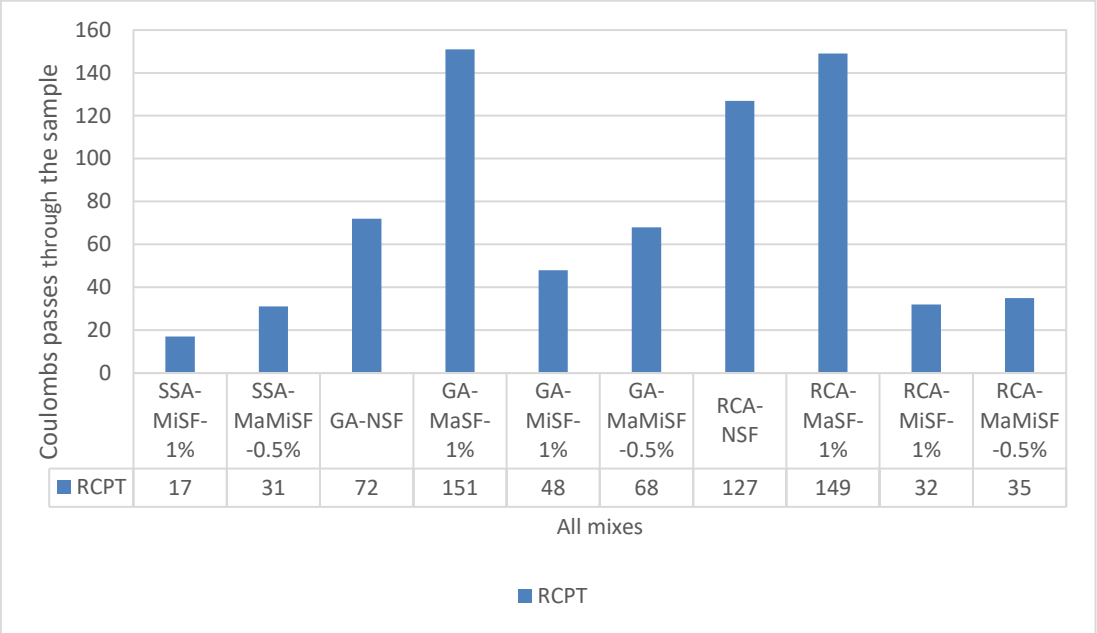

Figure 24. RCPT Values for All Samples

As shown in Figure 24, GA-MASF-1% and RCA-MASF-1% have the highest values of RCPT compared with other samples which are 150 coulombs approximately, whereas SSA-MISF-1% has the lowest value of RCPT with 17 coulombs only. When RCPT values are high, the chloride ion is more penetrated inside voids of the specimen, which leads to corrode steel fibers that affects the durability of UHPC in the future. In general, most samples have negligible values of RCPT except for GA-MASF-1%, RCA-NSF, and RCA-MASF-1%, according to the standard used for this test.

For control specimens, the value of RCPT in RCA-NSF is higher than the one in GA-NSF by 55 Coulombs, which means than the RCA without fibers allows for more chloride to pass through the specimen than GA. However, SSA-MISF-1% has lower RCPT value with a result of 17 Columbus. SSA-MISF-1% has a difference in RCPT values with GA-MISF-1% and RCA-MISF-1% by 31 Columbus and 15 Columbus, respectively, because SSA sample has lower void ratio than GA and RCA which leads

to a reduction in the number of coulombs that passes through the sample. GA-MASF-1% penetrates more chloride than GA-MISF-1%, GA-MAMISF-0.5% and GA-NSF by 103 Columbus, 83 Columbus and 79 Columbus, respectively. In general, samples with macro steel fibers allow more chloride to pass through the surface than the rest of the samples. On the other hand, samples with micro steel fibers have a lower possibility of corrosion in the future. As mentioned earlier, micro steel fiber increases the dense of the mix due to its small size.

Sorptivity

In this test, all samples are prepared to be 50 mm in height and dried in an oven until the difference between before and after heating is below 0.5%. The duration of this test is 28 days, and in certain times specified by the standard reading are recorded for each sample. The calculations depend on certain constant parameters, such as area exposed to water, which is equal to 7850 mm^2, and the temperature of water which is 18.8 degree Celsius that leads to having a density of water to be 998 Kg/m^3. In Table 12, initial and secondary absorptions of all UHPC mixes are shown. The initial absorption is the values taken from the first minute until 6 hours. For secondary absorption, the values are taken from day one until day 28. However, secondary absorption values do not follow linear relationship results and the figures show systematic curvature, therefore the secondary rate of absorption cannot be determined. This is due to the inconsistent values related to the balance used in this experimental work, which is measured to the nearest 0.1 g. Therefore, the initial rate of absorption is considered instead. Both initial and secondary absorption values are presented in the appendix.

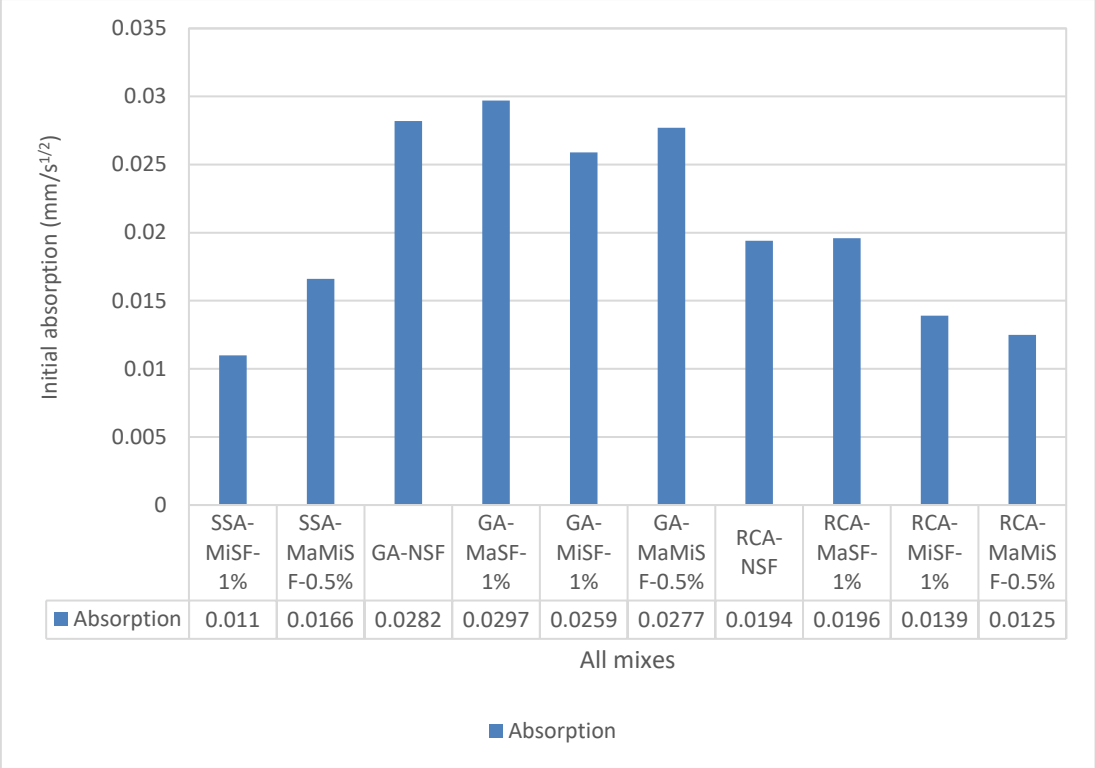

Figure 25. Initial Absorption Value for All Samples

As shown in Figure 25, the maximum initial absorption value is GA-MASF-1%, while the minimum is SSA-MISF-1%. The initial absorption rate is higher in GA-NSF compared to RCA-NSF. In general, GA samples have the highest initial absorption values, followed by RCA then SSA. As mentioned earlier, using GA without fibers increases water absorption more than RCA within 6 hours.

For RCA samples, the effect of adding steel macro fibers is insignificant compared to the control sample (RCA-NSF), and using micro steel fiber lowers the rate of water absorption. The highest rate is RCA-MASF-1%, followed by RCA-NSF, RCA-MISF-1%, and finally, RCA-MAMISF-0.5%. Therefore, using macro steel fibers increases the absorption rate. In general, the water absorption value depends on the porosity percentage of UHPC samples. When the porosity percentage is high, the absorption becomes high as well.

The Behavior of Combined Tests

The following section discusses the behavior of mechanical and durability properties combined for all UHPC mixes used in this research.

Compressive Strength Test vs. Porosity Results

Figure 26 represents the relationship between the compressive strength results of UHPC mixes with porosity tests at 28 days of curing.

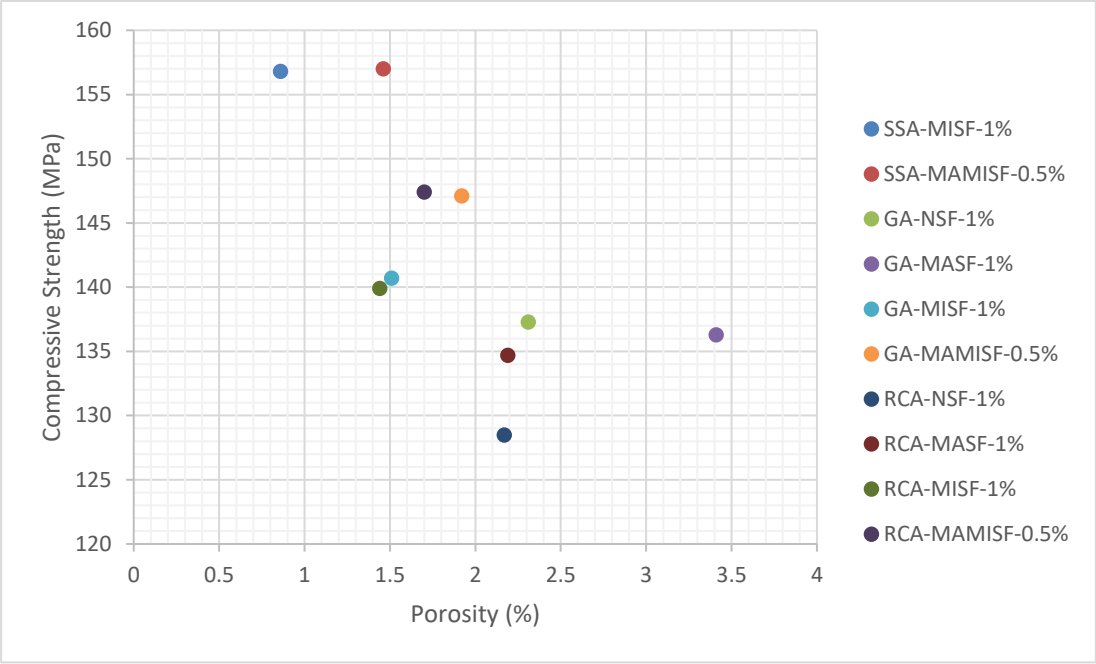

Figure 26. Relationship Between Compressive and Porosity Results

It is clearly shown that when the porosity percentage in UHPC sample is low the compressive strength is high, and vice versa. Therefore, the relationship between compressive strength and porosity percentage is inversely proportional. The lowest porosity percentage is SSA-MISF-1% with 0.86% and with a compressive strength of 156.8 MPa, which is considered one of the highest compressive strength results. Moreover, the highest porosity percentage is for GA-MASF-1% with 3.41% and has a

low compressive strength result with 136.3 MPa. It is noticed that for all samples with porosity less than 2% the compressive strength exceeds 140 MPa. All micro steel fiber samples have low percentage of porosity that enhance the results of compressive strength. However, using macro steel fiber produces UHPC samples with high voids volume which decreases the compressive strength results. Micro steel fiber is small in size compared to macro steel fiber which leads to reduction in the crack width and enhancement of the packing density of the mix. Finally using a combination of macro and micro steel fibers produces moderate pore volumes in specimens. In general, increasing the porosity percentage with 2.5% reduces the compressive strength by 13% approximately.

Electrical Resistivity vs. RCPT Results

The following figure shows the relationship between electrical resistivity test and RCPT.

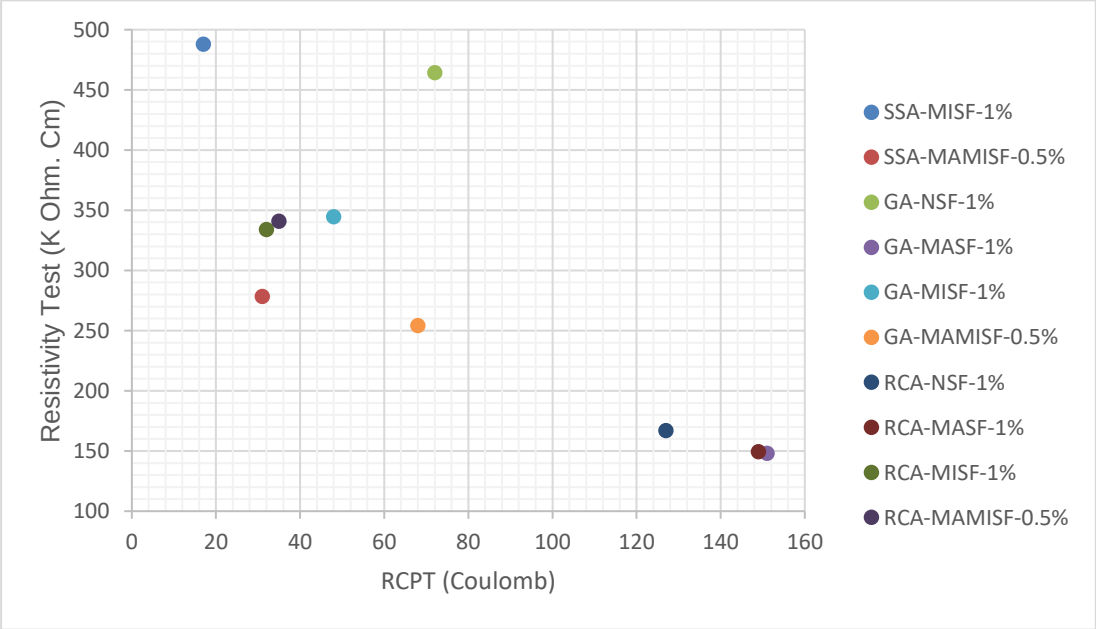

Figure 27. Relationship Between Electrical Resistivity and RCPT Results

It is observed from Figure 27 that the relationship is also inversely proportional. In fact, both tests results are the same because resistivity measures the resistance of chloride penetration ions through UHPC samples and RCPT measures the transfer of a charge through UHPC surface. In addition, both tests measure the quality of UHPC and give an indicator of the easily corrodible steel fibers. While resistivity test follows the AASHTO-TP-95 standard and tests the sample easily and quickly, the standard for RCPT test is C-1202 and is performed in labs after a lengthy process. SSA-MISF-1% sample has the lowest RCPT value (17 coulombs) and the highest resistivity result (487.88 kohm.cm). SSA with micro steel fibers produces a dense mix that has a low porosity volume and micro steel fiber has a small size which makes the effect of conducting the charges and ions is negligible. GA-MASF-1% and RCA-MASF-1% share approximately the same results, where they have the lowest resistivity of about 150 kohm.cm and the highest RCPT with 150 coulombs. This is due to the fact that large size and number of fibers per unit volume of UHPC enables fibers to pass the charges easily in the sample.

Porosity Test vs. Sorptivity Results

As shown in Figure 28, porosity and initial absorption tests have a proportional relationship; when the porosity increases the rate of water absorption increases in the specimen and vice versa. GA-MASF-1% has the highest value of porosity and Sorptivity test (3.41% and 0.0297 $mm/s^{1/2}$). The lowest value of both porosity and initial absorption is SSA-MISF-1% (0.86% and 0.011 $mm/s^{1/2}$) which are considered good properties to avoid keeping water in the voids, as well as it creates charge conduction to allow the steel fibers to be corroded which leads to a decrease in the compressive strength results. As mentioned before, the high porosity percentage is caused by large particles. Since macro steel fiber is larger than micro steel fiber, more cracks width

appears in specimen which makes the absorption of water easily by capillarity suction. The combination of fibers provides moderate pores and initial water suction rate. In general, increasing the void percentage with approximately 2.5% increases the rate of water absorption by 170%.

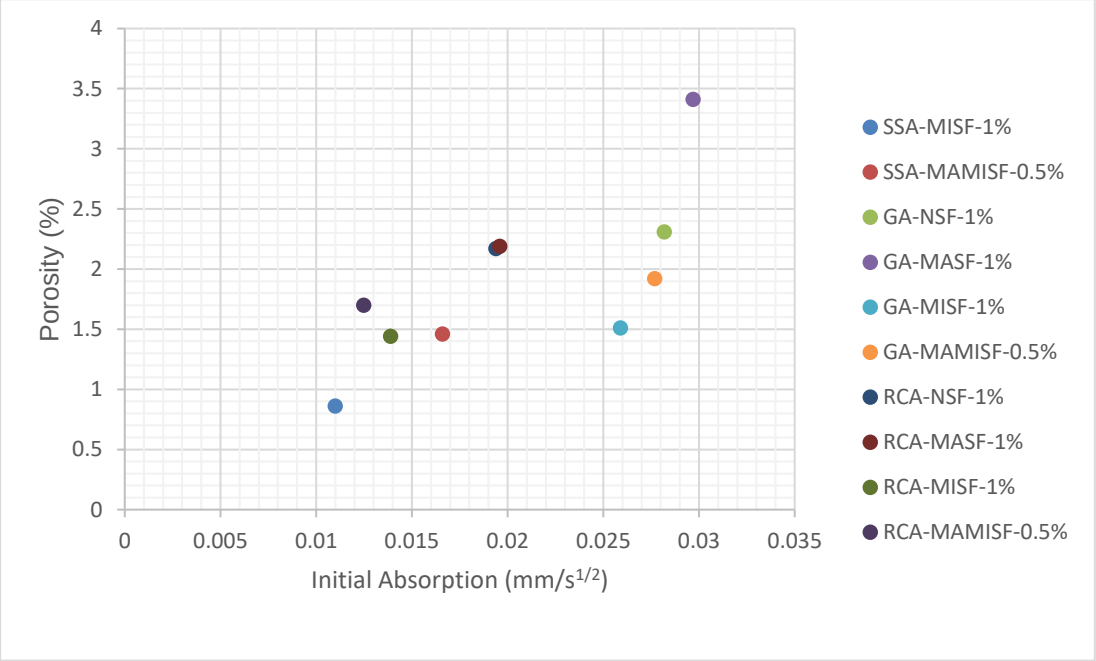

Figure 28. Relationship Between Porosity and Sorptivity Results

Summary of Mechanical and Durability properties

SSA has the highest compressive and flexural strengths and durability due to higher specific gravity, their extensive pore network, and substantial rough surface, which creates a dense Interfacial Transition Zone (ITZ) between the aggregate and its surrounding components and provides a better interlocking. GA has high mechanical properties due to its angular shape which provides good interlocking. On the other hand, RCA has low mechanical properties because of crashed aggregate after demolishing structure creates poor mortar layer on the surface. Micro steel fibers provide denser mix and do not cause much pores which enhances compressive and durability behaviors.

Macro steel fiber provides better bridging behavior where its length and width reduce the propagation of cracks leading to an increase in the value of flexural strength.

For durability tests, the lower the volume of pores, the better durability results are. As previously discussed, micro steel fiber and SSA provide low volume of voids which result in a low rate of water absorption, a low amount of chloride passes through samples, and a high resistivity for electricity. Macro steel fiber causes void volumes to increase, in addition to the increase of water absorption rate and the possibility of fiber corrosion. For the combination of both micro and macro steel fiber sample, it provides a moderate durability behavior which falls between separately using micro steel fiber or macro steel fiber.

CHAPTER 5: CONCLUSION

UHPC is a new generation of concrete that can significantly enhance both the mechanical and durability properties of reinforced concrete structural members. In this research, the focus is to use coarse aggregates with a size up to 10 mm to produce UHPC with locally available concrete materials in the State of Qatar. The significance of this study is to investigate the mechanical properties (compressive and flexural tensile strengths) and the durability behavior of the produced UHPC. Finally, to study the influence of the type of aggregates and fibers on the mechanical properties and the durability of UHPC. The summary of this master thesis is as follow:

- Using silica fume and fly ash in the mix enhances the compressive strength and durability of UHPC mixes.
- The total number of trial mixes are 12 divided into 3 trials for each type of aggregate, where each trial has different volumes of fiber such as control sample (0%), 1% of macro steel fibers, 1% of micro steel fibers, and 0.5% of both macro and micro steel fibers. Fibers improve the flexural tensile strength.
- For compressive strength, using SSA provides the best values of compressive strength compared with GA and RCA, due to their heavier specific gravity, large pore network and substantial rough surface. These large pores impact the Interfacial Transition Zone (ITZ) by supporting creating a dense ITZ between the aggregate and its surrounding components. The rough aggregate surface provides better interlocking with the UHPC component.
- The improved strength of GA makes it the second-best aggregate after SSA in terms of compressive strength, because of its angularity produces enhanced interlocking compared to RCA. Hence, RCA produced the least compressive strengths at the same mixture proportions compared to GA and SSA. Such strengths affected by the

additional poor mortar layer after demolishing the old structure.

- The combination of both macro and micro steel fibers in concrete mixes resulted in the highest values of compressive strength for all types of aggregate, followed by the micro steel fibers, then macro steel fibers, and finally the control mixes with no fibers being utilized. Such improvement in compression strength can be linked to its ability to stop extending microcracks available in the UHPC. Although it has a positive impact on compressive strength and flexural tensile strength, the enhancement in the flexural strength is significantly better than the compressive strength.
- All mixes increase the compressive strength of about 20 MPa after 28 days of curing than 7 days due to the hydration process.
- Both SSA-MISF-1% and SSA-MAMISF-0.5% reach more than 150 MPa after 28 days of curing. The significant improvement in the results is for mixes that use micro steel fibers samples and 0.5% of micro and macro steel fibers samples.
- For flexural strength, SSA and GA produce better results in flexural tensile strength than RCA. These improvements are related to their dense ITZ that supports the transfer of stresses from UHPC matrix to aggregates. The higher mechanical interlocking is also a significant factor in improving the stress transfer and the flexural strength of UHPC.
- It is noticed that using mixes with the absence of fiber makes the aggregate easier to break without any signs, which means including fibers in the mix provides much better flexural tensile strength.
- Utilizing macro steel fibers in the mix achieves better flexural tensile strength than using both micro and macro and finally, micro steel fiber due to the fiber's high tensile strength and large size of aggregate. This development is attributed to the improvement of ITZ that the fibers impose, the reduction of cracks widening, and the distribution of stresses away from the ITZ.

- The flexural behavior for all samples increases the load with the displacement control of 0.1 mm/min until it reaches the maximum loading, then the plastic limit starts, and some cracks appear in prisms. For control samples, they break directly when it reaches that stage. For samples that have steel fibers, the load decreases steeply then slightly decreases until the samples break.
- The electrical resistivity test represents the quality of the material used and it gives a good indication that it is durable and sustainable. If the result of this test is high, then the risk of corrosion becomes low. Using silica fume and fly ash plays an essential role in having good electrical resistivity results.
- For electrical resistivity, using SSA with micro steel fibers has the highest value since the mix has low porosity percentage which lead to reduce the amount of water absorption. Then, the electrical resistivity will be high.
- For the porosity test, the maximum porosity percentage is for GA with the use of 1% of macro steel fibers with a 3.41% of sample volume. The lowest percentage of porosity is for SSA with the use of 1% of micro steel fibers with a percentage of 0.86% of sample volume.
- In general, SSA specimens have less pores than GA and RCA due to good ITZ. In addition, using macro steel fibers increases the percentage of pores in samples since it is long and the interaction between aggregate and macro fibers is weak. For the same reason, using micro steel fibers can have lower voids than specimens containing macro steel fibers.
- Samples GA-MASF-1% and RCA-MASF-1% have the highest value of RCPT compared with other samples which is 150 coulombs approximately. Moreover, the lowest value of RCPT is seen in SSA-MISF-1% with 17 coulombs. When RCPT values are high, the chloride ion passes more inside voids of specimen, which leads to having

corrosion that can affect the durability of UHPC in future. In general, most of the samples had negligible values of RCPT except GA-MASF-1%, RCA-NSF and RCA-MASF-1.

- SSA results are the lowest regarding RCPT values. Also, the ability to resist the penetration of chloride ions in micro steel fibers is more than macro steel fibers.
- For sorptivity test, the maximum initial absorption value is GA-MASF-1%, GA with macro steel fibers. The minimum initial absorption value is SSA-MISF-1%, which is SSA with the use of 1% of micro steel fibers.
- Porosity and compressive strength relationship is inversely proportional, when the porosity percentage in UHPC sample is low the compressive strength is high and when the porosity percentage is high, then the compressive strength is low.
- The relationship between electrical resistivity and RCPT is inversely proportional. Actually, both tests results are the same, because resistivity measures the resistance of chloride penetration ions through UHPC samples and RCPT measures the transfer of a charge through UHPC surface. Resistivity test has different standard (AASHTO TP 95) and can test the sample easily and quickly. The standard of RCPT is C-1202 and it should perform in lab after lengthy process.
- porosity and initial absorption tests have directly proportional relationship. If the porosity increases, then rate of water absorption increases in the specimen.
- It is noticed that compressive strength, electrical resistivity, RCPT and Sorptivity tests are directly affected by porosity percentage of the sample.

Recommendations for Future Research

- Use coarse aggregate with size more than 10 mm is a good research work for future researchers.
- Utilize different types of a synthetic with plastic and other metallic fibers to improve the ductility of UHPC.
- Study the effect of fiber orientations in UHPC and how it can be affected by their properties.
- Involve more durability tests such as sulfate attack, alkali-silica reaction, freeze-thaw, cavitation, and expansion.

REFERENCES

1. Dunn, R. C., Ross, R. A., and Davis, G. D. (2010). “Corrosion monitoring of steel reinforced concrete structures using embedded instrumentation.” NACE Corrosion Conf. and Expo, NACE International, San Antonio, TX, 1–10.
2. Fehling, E. M. S. (2004). “Ultra high-performance concrete (UHPC).” Proc., Int. Symp. on Ultra High-Performance Concrete, Kassel University Press, Kassel, Germany.
3. Wille, K. (2013). “Development of non-proprietary ultra-high-performance concrete for use in the highway bridge sector.” Rep. No. PB2013-110587, National Technical Information Service, Springfield, VA.
4. Wille, K., Naaman, A. E., and Parra-Montesinos, G. J. (2011c). “Ultra-high-performance concrete with compressive strength exceeding 150 MPa (22 ksi): A simpler way.” ACI Mater. J., 108(1), 46–54.
5. Habel, K., Viviani, M., Denarié, E., and Brühwiler, E. (2006). “Development of the mechanical properties of an ultra-high-performance fiber reinforced concrete (UHPFRC).” Cem. Concr. Res., 36(7), 1362–1370.
6. Mehta, P. K., and Monteiro, P. J. M. (2006). Concrete: Microstructure, properties, and materials, McGraw-Hill, New York.
7. Powers, T. C. (1958). “Structure and physical properties of hardened Portland cement paste.” J. Am. Ceram. Soc., 41(1), 1–6.
8. C.K. Park, M.H. Noh, T.H. Park, Rheological properties of cementitious materials containing mineral admixtures, Cem. Concr. Res. 35 (5) (2005) 842–849.
9. P.Y. Blais, M. Couture, Precast, prestressed pedestrian bridge - World's first reactive powder concrete structure, Pci J, 44 (1999) 60-71.

10. B.A. Graybeal, Ultra-High-Performance Concrete, FHWA-HRT-13-060, The Federal Highway Administration, McLean, VA, 2011.
11. S. Mindess, J.F. Young, D. Darwin, Concrete, 2nd ed., Prentice Hall, Upper Saddle.
12. E. Sakai, K. Aizawa, A. Nakamura, H. Kato, M. Daimon, Influence of superplasticizers on the fluidity of cements with different amount of aluminate phase, Second International Symposium on Ultra High-Performance Concrete, 2008, pp. 85-92.
13. P.R. Rangaraju, H. Kizhakommudom, Z. Li, S.D. Schiff, Development of High-Strength/High Performance Concrete/Grout Mixtures for Application in Shear Keys in Precast Bridges, FHWA-SC-13-04a, FHWA, U.S. Department of Transportation, 2013.
14. Bache, H. H. (1981). "Densified cement/ultra fine particle-based materials." 2nd Int. Conf. on Superplasticizers in Concrete, Aalborg Portland, Ottawa.
15. Richard, P., and Cheyrezy, M. (1995). "Composition of reactive powder concretes." Cem. Concr. Res., 25(7), 1501–1511.
16. Buitelaar, P. (2004). "Ultra high-performance concrete: Developments and applications during 25 years." Int. Symp. on UHPC, Iowa State Univ., Ames, IA.
17. Dils, J., De Schutter, G., and Boel, V. (2012). "Influence of mixing procedure and mixer type on fresh and hardened properties of concrete: A review." Mater. Struct., 45(11), 1673–1683.
18. Graybeal, B. A. (2006). "Material property characterization of ultra-high-performance concrete." FHWA Rep. No. FHWA-HRT-06-103, Federal Highway Administration Research and Technology, Turner-Fairbank Highway

Research Center, McLean, VA.

19. Yu, R., Spiesz, P., and Brouwers, H. J. H. (2015). “Development of ultrahigh performance fibre reinforced concrete (UHPFRC): Towards an efficient utilization of binders and fibres.” Construct. Build. Mater., 79, 273–282.
20. Shi, C., Wu, Z., Lv, K., and Wu, L. (2015). “A review on mixture design methods for self-compacting concrete.” Constr. Build. Mater., 84, 387–398.
21. P.R. Rangaraju, H. Kizhakommudom, Z. Li, S.D. Schiff, Development of High-Strength/High Performance Concrete/Grout Mixtures for Application in Shear Keys in Precast Bridges, FHWA-SC-13-04a, FHWA, U.S. Department of Transportation, 2013.
22. Sobuz, H. R., Visintin, P., Mohamed Ali, M. S., Singh, M., Griffith, M. C., and Sheikh, A. H. (2016). “Manufacturing ultra-high performance concrete utilising conventional materials and production methods.” Constr. Build. Mater., 111, 251–261.
23. Chen, Y., Matalkah, F., Soroushian, P., Weerasiri, R., & Balachandra, A. (2019).
24. Alsalman, A., Dang, C.N., & Hale, W.M. (2017).
25. Pierard, J., Dooms, B., & Cauberg, N. (2012). Evaluation of durability parameters of UHPC using accelerated lab tests. In Proceedings of the 3rd International Symposium on UHPC and Nanotechnology for High Performance Construction Materials, Kassel, Germany (pp. 371–376).
26. El-Dieb, A. S. (2009). “Mechanical, durability and microstructural characteristics of ultra-high-strength self-compacting concrete incorporating steel fibers.” Mater. Des., 30(10), 4286–4292.
27. Plank, Johann et al. 2009. “Effectiveness of Polycarboxylate Superplasticizers

in Ultra-High Strength Concrete: The Importance of PCE Compatibility with silica fume.” 7(1): 5–12.

28. Vernet, P. (2004). Ultra-durable concretes: Structure at the micro- and nanoscale. Mater Res Soc, 29(5), 324–327.
29. Roux, N., Andrade, C., & Sanjuan, M. (1996). Experimental study of durability of reactive powder concretes. Journal of Materials in Civil Engineering, 8(1), 1–6.
30. Wang, Chong et al. 2012. “Cement & Concrete Composites Preparation of Ultra-High-Performance Concrete with Common Technology and Materials.” Cement and Concrete Composites 34(4): 538–44. http://dx.doi.org/10.1016/j.cemconcomp.2011.11.005.
31. Kim Y, Lee K, Bang J, Kwon S 2014 Adv Mater Sci Eng 1–12.
32. Gao, R., Liu, Z., Zhang, L., & Stroeven, P. (2006). Static properties of reactive powder concrete beams. Key Engineering Materials, 302(303), 521–527.
33. Polder, R., C. Andrade, B. Elsener, Ø. Vennesland, J. Gulikers, R. Weidert, and M. Raupach. 2000. “Test methods for onsite measurement of resistivity of concrete.” Mater. Struct. Res. 33 (10): 603–611. https://doi .org/10.1007/BF02480599.
34. Mohamed O, Ati M, Al Hawat W, 2015 Using neural networks to predict chloride penetration of sustainable self-consolidating concrete, Civil-Comp Press.
35. S. Iffat, T. Manzur, M. Noor, "Durability performance of internally cured concrete using locally available low cost LWA", KSCE Journal of Civil Engineering, Vol. 21, p. 1256, 2017 DOI: https://doi.org/10.1007/s12205-016-0793-x.

36. Do-Young Moon, January 2013 Journal of the Korea institute for structural maintenance inspection 17(1):106-113 DOI: 10.11112/jksmi.2013.17.1.106
37. Dias, W. P. S. 2013. “Reduction of concrete sorptivity with age through carbonation.” Concr. Res. 30 (8): 1255–1261.
38. Patel, V. N. 2009. Sorptivity testing to assess durability of concrete against freeze-thaw cycling. Montreal: Dept. of Civil Engineering and Applied Mechanics McGill Univ.
39. Zhang, S.P. and Zong, L. (2014) Evaluation of Relationship between Water Absorption and Durability Ofconcrete Materials. Advances in Materials Science and Engineering, 2014, Article ID: 650373 https://doi.org/10.1155/2014/650373.
40. O. Bonneau, P. C. Aïtcin: Determination of the coefficient of thermal expansion of high-performance concrete from initial setting. In: Materials and Structures, Vol. 35, S. 35-41, January 2002.
41. Willey, J. (2013). “Use of ultra-high-performance concrete to mitigate impact and explosive threats.” Master’s thesis, Missouri Univ. of Science and Technology, Rolla, MO.
42. Wong, H. H. C., and Kwan, A. K. H. (2008). “Packing density of cementitious materials. Part 1—Measurement using a wet packing method.” Mater. Struct., 41(4), 689–701.
43. Huo, X., and Wong, L. (2000). Early-age shrinkage of HPC decks under different curing methods, ASCE, Philadelphia.
44. Li, H., Liu, G. (2013). Tensile properties of hybrid fiber reinforced reactive powder concrete after expose to elevated temperature. International Journal of concrete Structures and Materials, 1–9.

45. Ma, J., & Schneider, H. (2002). Properties of ultra-high-performance concrete. Leipzig Annual Civil Engineering Report (LACER), 7, 25–32.
46. Ibrahim, Mustapha et al. 2017. “Effect of Material Constituents on Mechanical and Fracture Mechanics Properties of Ultra- High-Performance Concrete Effect of Material Constituents on Mechanical and Fracture Mechanics Properties of Ultra-High-Performance Concrete.”.
47. Yoo, Doo-yeol, and Nemkumar Banthia. 2016. “Mechanical Properties of Ultra-High-Performance Fiber-Reinforced Concrete: A Review.” Cement and ConcreteComposites73:267–80. http://dx.doi.org/10.1016/j.cemconcomp.2016.08.001.
48. Randl, N et al. 2014. “Development of UHPC Mixtures from an Ecological PointofView.” Construction and Building Material. http://dx.doi.org/10.1016/j.conbuildmat.2013.12.102.
49. Brühwiler, Eugen, Ecole Polytechnique, Fédérale Epfl, and Emmanuel Denarié. 2008. “Rehabilitation of Concrete Structures Using Ultra-High Per- Formance Fibre Reinforced Concrete.” (1): 1–8.
50. Cwirzen, A. (2007). The effect of the heat-treatment regime on the properties of reactive powder concrete. Advances in Cement Research, 19(1), 25–33.
51. K. Wille, A.E. Naaman, G.J. Parra-Montesinos, Ultra-High-Performance Concrete with Compressive Strength Exceeding 150 MPa (22 ksi): A Simpler Way, Aci Mater J, 108 (2011) 46-54.
52. Wu, Zemei, Caijun Shi, Wenhe, and Linmei Wu. 2016. “Effects of Steel Fiber Content and Shape on Mechanical Properties of Ultra High-Performance Concrete.” Construction and Building Materials 103: 8–14. http://dx.doi.org/10.1016/j.conbuildmat.2015.11.028.

53. Kang, Su-tae, Yun Lee, Yon-dong Park, and Jin-keun Kim. 2010. “Tensile Fracture Properties of an Ultra High-Performance Fiber Reinforced Concrete (UHPFRC) with Steel Fiber.” Composite Structures92(1):617. http://dx.doi.org/10.1016/j. compstruct.2009.06.012.
54. Kazemi, Sadegh, and Adam S Lubell. 2013. “Influence of Specimen Size and Fiber Content on Mechanical Properties of Ultra-High-Performance Fiber-Reinforced Concrete.” (109).
55. Maca, P., Zatloukal, J., and Konvalinka, P. (2012). “Development of ultra high-performance fiber reinforced concrete mixture.” IEEE Symp. On Business, Engineering and Industrial Applications (ISBEIA), IEEE, New York, 861–866.
56. Alkaysi, M., and El-Tawil, S. (2015). “Structural response of joints made with generic UHPC.” Proc., Structures Congress 2015, ASCE, Reston, VA, 1435–1445.
57. Azad, A. K., and Hakeem, I. Y. (2013). “Flexural behavior of hybrid concrete beams reinforced with ultra-high-performance concrete bars.” Constr. Build. Mater., 49, 128–133.
58. Ma, J., & Schneider, H. (2002). Properties of ultra-high-performance concrete. Leipzig Annual Civil Engineering Report (LACER), 7, 25–32.
59. Grand View Research (GVR). Ultra-High-Performance Concrete (UHPC) Market Analysis by Product, By Application, And Segment Forecasts 2014 – 2025. 2017.
60. Y.L. Voo, W.K. Poon, Ultra-High-Performance ductile concrete (UHPC) for Bridge engineering, Proceedings of the International Conference and Exhibition on Bridge Engineering (2009).
61. M. Schmidt, E. Fehling, Ultra-High-Performance concrete: research

development and application in Europe, The 7th International Symposium on the Utilization of High-Strength/High-Performance Concrete (2005) 51–78.

62. P.Y. Blais, M. Couture, Precast, prestressed pedestrian Bridge - world's first reactive powder concrete structure, PCI J. 44 (5) (1999) 60–71.
63. P. Acker, M. Behloul, Ductal1 technology: a large spectrum of properties, ultra-High-Performance concrete, Kassel, Germany (2004) 11–23.
64. J. Resplendino, First recommendations for ultra-High-Performance concretes and examples of application, Proceedings of the International Symposium on Ultra-High-Performance Concrete (2004) 79–89.
65. Z. Hajar, A. Simon, D. Lecointre, J. Petitjean, Design and construction of the world first ultra-High-Performance Road Bridges, Proceedings of the International Symposium on Ultra-High-Performance Concrete (2004) 39–48.
66. M. Behloul, K.C. Lee, Ductal! Seonyu footbridge, Struct. Concr. 4 (4) (2003) 195–201.
67. F. Toutlemonde, J. Resplendino, Designing and Building With UHPFRC: State of the Art and Development, ISTE, London, 2011.
68. T. Zdeb, UHPC - properties and technology. Bulletin of the Polish academy of sciences, Tech. Sci. 61 (1) (2013) 183–193.
69. S. Aubry, P. Bompas, B. Vaudeville, D. Corvez, T. Lagrange, P. Mazzacane, A. Brizou, A UHPFRC cladding challenge: the fondation Louis vuitton pour La creation ‘Iceberg’, Proceedings of International Symposium on Ultra-High-Performance Fiber Reinforced Concrete (2013) 37–48.
70. P. Menetrey, UHPFRC cladding for the Qatar national Museum, Proceedings of International Symposium on Ultra-High-Performance Fiber-Reinforced Concrete (2013) 351–360.

71. P. Mazzacane, R. Ricciotti, F. Teply, E. Tollini, D. Corvez, MUCEM: the builder's perspective, Proceedings of International Symposium on Ultra-High-Performance Fiber Reinforced Concrete (2013) 3–16.
72. R. Fabbri, D. Corvez, Rationalisaztion of complex UHPFRC façade shapes, Proceedings of International Symposium on Ultra-High Performance FiberReinforced Concrete (2013) 27–36.
73. Z. Hajar, M. Novarin, C. Servant, G. Genereux, D. Przybyla, D. Bitar, Innovative solution for strengthening orthotropic decks using UHPFRC: the illzach Bridge, Proceedings of International Symposium on Ultra-High-Performance Fiber-Reinforced Concrete (2013) 117–126.
74. L. Moreillon, P. Menetrey, Rehabilitation and strengthening of existing RC structures with UHPFRC: various applications, Proceedings of International Symposium on Ultra-High-Performance Fiber-Reinforced Concrete (2013) 127–136.
75. T. Ono, Application of UHSFRC for Irrigation Chanel Repair Works. Designing and Building With UHPFRC—State of the Art and Development, ISTE Ltd., London, 2011, pp. 541–552.
76. Wang, J. et al. (2018) Combining life cycle assessment and BIM to account for carbon emission of building demolition waste. J. Clean Prod. 172, 3154-66.
77. Zheng, L., et al. (2017). Characterizing the generation and flows of construction and demolition waste in China. Constr. Build. Mater., 136, 405-13.
78. Wu et al. (2019). A review of performance assessment methods for construction and demolition waste management. Resour. Conserv. Recy. 150, 104407.
79. MDPS (Ministry of Development Planning and Statistics (2014). Environment Statistics Annual Report 2013 (2008–2012). www.mdps.gov.qa.

APPENDIX A: ABSORPTION FOR CONTROL MIXES

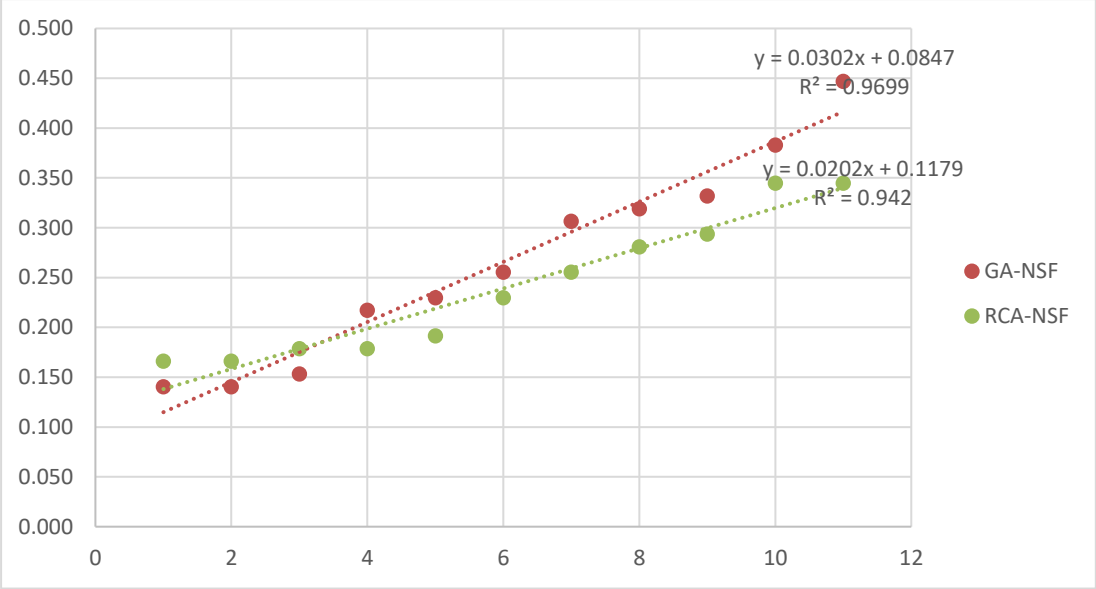

Figure 29. Initial Absorption for Control Mixes

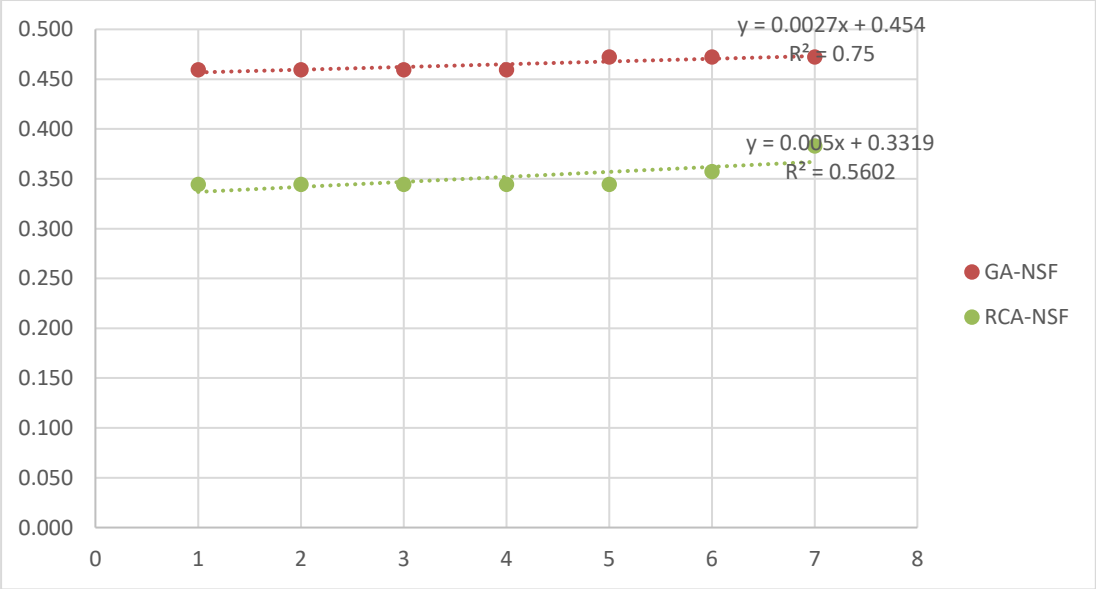

Figure 30. Secondary Absorption for Control Mixes

APPENDIX B: ABSORPTION FOR MACRO STEEL FIBERS

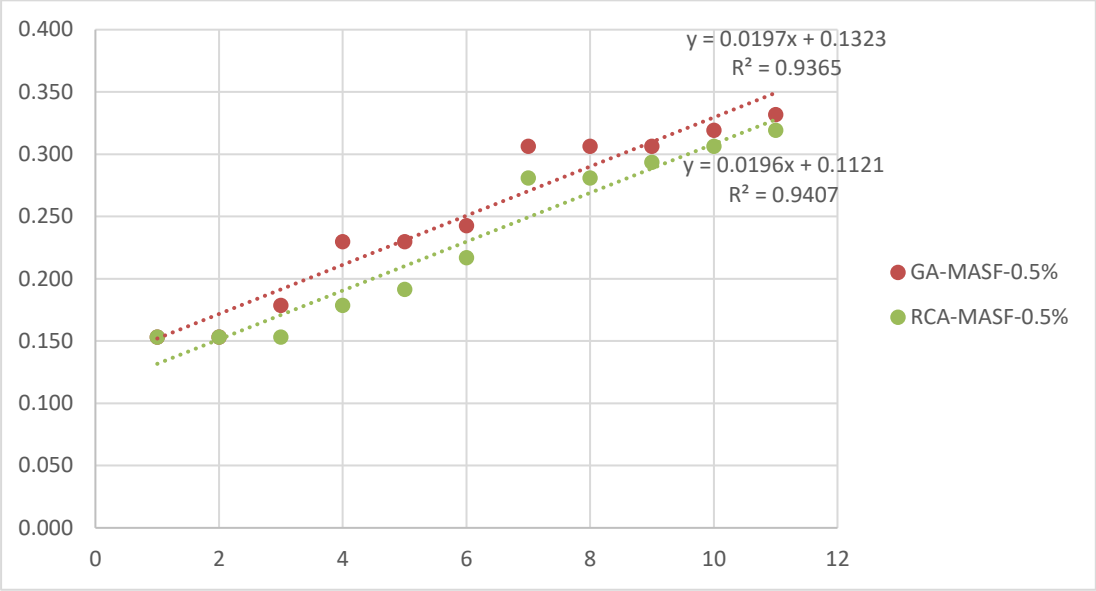

Figure 31. Initial Absorption for Macro Steel Fibers

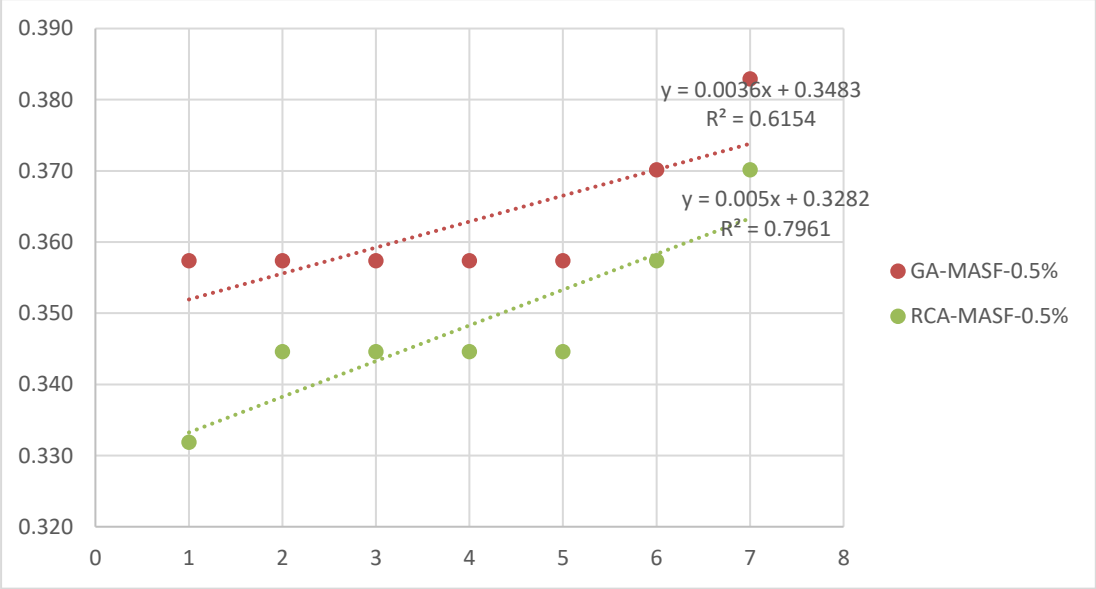

Figure 32. Secondary Absorption for Macro Steel Fibers

APPENDIX C: ABSORPTION FOR MICRO STEEL FIBERS

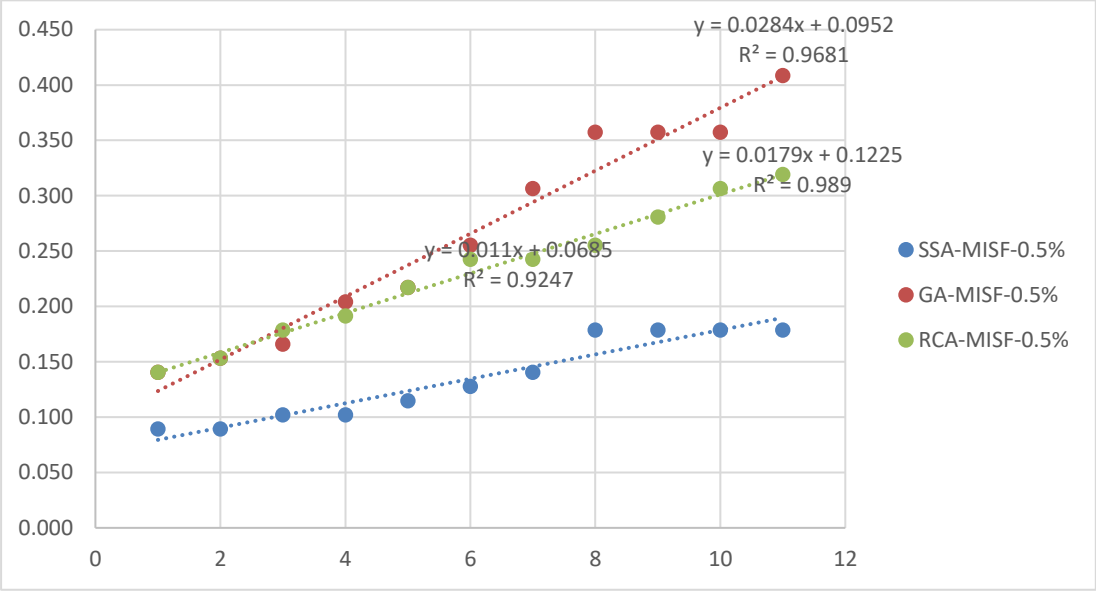

Figure 33. Initial Absorption for Micro Steel Fibers

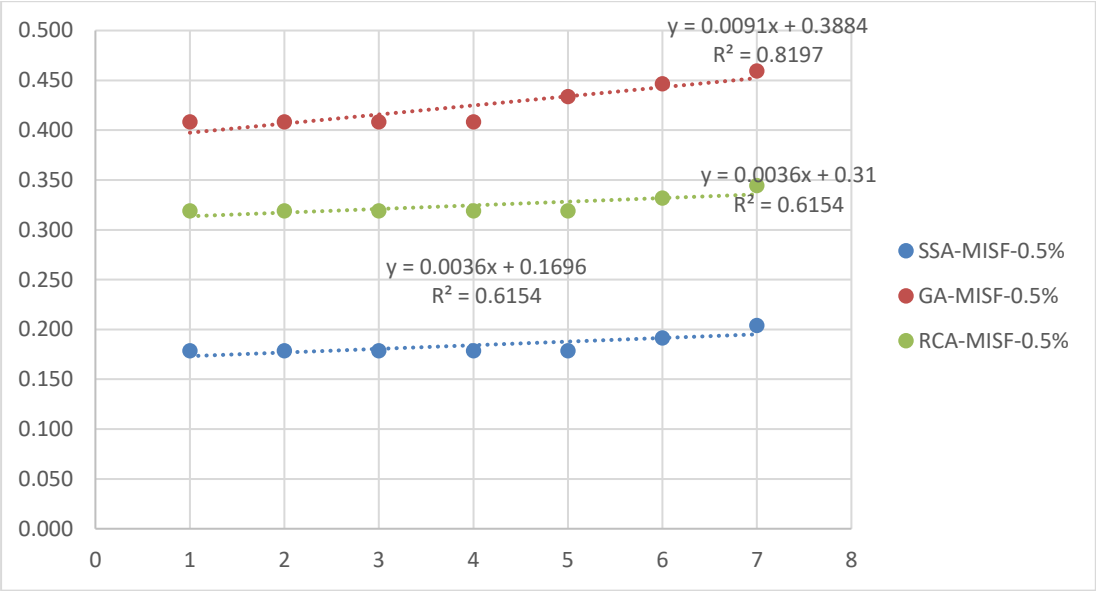

Figure 34. Secondary Absorption for Micro Steel Fibers

APPENDIX D: ABSORPTION FOR MICRO AND MACRO STEEL FIBERS

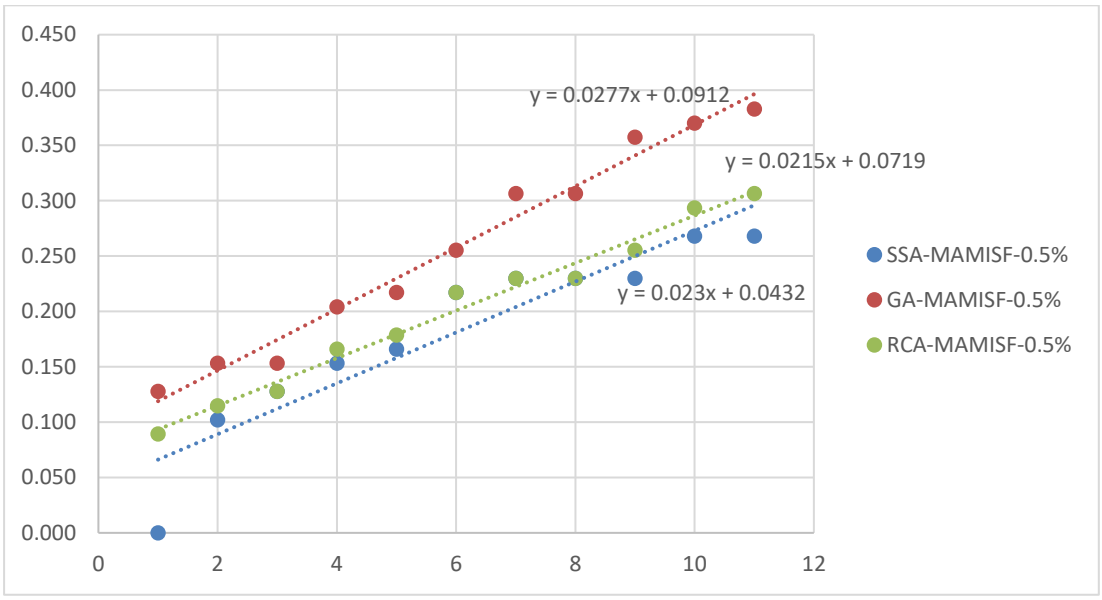

Figure 35. Initial Absorption for Micro and Macro Steel Fibers

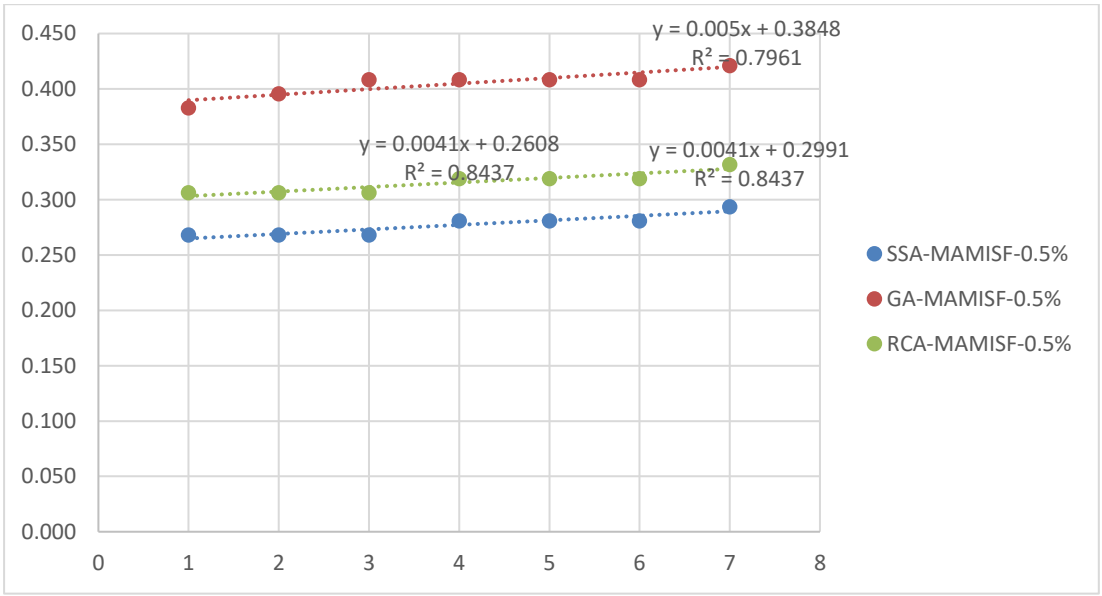

Figure 36. Secondary Absorption for Micro and Macro Steel Fibers